EVALUATING THE POTENTIAL OF ULTRASHORT SELF-ASSEMBLING PEPTIDES SCAFFOLDS AS SUITABLE 3D MATRICES FOR ORGANOID FABRICATION

Alexandra Antunes

MASTER THESIS IN CHEMICAL ENGINEERING

presented to the Faculty of Engineering of the University of Porto

Developed within the course of dissertation held in KAUST, Laboratory for Nanomedicine

Supervisor at FEUP: Prof. Maria do Carmo Pereira

Supevisor at KAUST: Charlotte Hauser

Porto, July 2023

"الصبر مفتاح الفرج"

Acknowledgment

As one of the most fulfilling journeys of my life, it's time to give back to those who gave me.

First and foremost, I want to leave an appreciation note to my supervisors Prof. Maria do Carmo Pereira and Prof. Charlotte Hauser. It is thanks to their belief in my abilities and the opportunity they provided me that I was able to fulfill this thesis journey. I am deeply grateful to Shireen Abdelrahman, for her patience, assistance, kindness throughout the entire process and for teaching me valuable lessons that extend beyond academia. To this exceptional person and professional, and I feel fortunate to have had the opportunity to find your path. To my professors who have imparted their knowledge to me over the course of these five years, I offer my sincere appreciation. I would also like to thank the DEQ for all the services and opportunities abroad.

My heartfelt thanks go to my family, particularly my parents, for their incommensurable support in all my most unconventional decisions. I would also like to express my gratitude to my brother, the dearest person to my heart, with whom I shared four transformative years. His positivity, kindness, and love have been a constant source of inspiration.

I am truly grateful for the incredible friendships I have cultivated during my university years. To "Onde bamos," thank you for the amazing moments we shared together. A special mention goes to Marta, whose unwavering support have pushed me to reach new heights. A heartfelt thank you goes to my roommate, Mariano, who has been a constant source cheer during those last years. I would also like to express my gratitude to the friends I made during my last year abroad, in Hong Kong, to my roommate, Carolina, my dear friend Cyrine and Harsh, your companionship and shared experiences made my journey even more memorable. To my friends from Saudi Arabia, especially Aris, Khadija, Angelly, Thomas, and Amina, thank you for making this experience unique. I also want to express my appreciation for the hospitality and kindness of all my Saudi friends and their beautiful country. To the beautiful souls that have shaped my academic journey and personal growth, and I am deeply indebted to them all.

Abstract

This thesis focuses on the evaluation of selected self-assembling ultrashort peptides as potential scaffolds for 3D organoid development. The suitability of three newly designed tetrameric self-assembling peptide hydrogels was assessed: PEP1, PEP2, PEP2-RGD. Mechanical characterization of the peptide hydrogels was performed to determine their elasticity and stiffness. Their ability to provide a supportive and biomimetic environment for cells was evaluated with three cell types: HDFs, HEK293 and SH-SY5. Cell viability within the peptide hydrogels was assessed by live-dead cell assays, ATP assays, and cytoskeleton imaging techniques. The results demonstrated that the selected peptides hydrogels supported cell viability and maintained cellular function, indicating their potential as suitable scaffolds for 3D organoid culture. Furthermore, the peptide hydrogels were evaluated for their compatibility with bioprinting technology. Successful fabrication of cell-laden scaffolds using the selected peptide hydrogels was achieved, highlighting their applicability in advanced tissue engineering approaches.

Keywords: organoids – 3D bioprinting – 3D cell culture – self-assembling - ultrashort peptides – hydrogel – rheology – cellular viability - biomaterials – bioprinting – tissue engineering

Resumo

Esta tese tem como objetivo avaliar o potencial de peptídeos ultracurtos e auto-organizáveis (SAPs), como blocos formadores de hidrogéis, destinados ao desenvolvimento de organoides tridimensionais. Os SAPs são biomateriais compostos por aminoácidos naturais, com propriedades únicas de biocompatibilidade, auto-organização, reprodutibilidade e versatilidade. As suas propriedades de biodegradabilidade, mecânicas e efeitos anti-microbianos são ajustáveis, presentando uma grande vantagem em relação a materiais habitualmente usados. Avaliamos quatro hidrogéis à base de SAPs (PEP1, PEP2, PEP2-RGD) quanto às suas propriedades mecânicas, suporte à viabilidade e função celular, e compatibilidade com a tecnologia de bioimpressão por extrusão.

Primeiro, testamos as propriedades mecânicas dos hidrogéis através de testes de gelificação e medidas reológicas para determinar elasticidade e rigidez. De seguida, avaliamos a compatibilidade com células usando três linhagens celulares diferentes (HDFs, HEK293 e SH-SY5). Os ensaios de viabilidade celular incluíram coloração, quantificação de ATP e imagiologia do citoesqueleto. Os resultados demostraram que os hidrogéis selecionados suportaram a as funções celulares e mantiveram as suas viabilidades comprovando o seu potencial como suporte para cultura de organoides 3D. Os hidrogéis foram também avaliados como material para impressão tridimensional, e foram extrudidas bioconstruções usando os com resultados favoráveis nos testes prévios.

Este estudo contribuiu para o avanço dos biomateriais destinados ao desenvolvimento de organoides tridimensionais, oferecendo mais oportunidades para desenvolver organoides mais fidedignos aos tecidos vivos. Adicionalmente, esses novos materiais podem ser aplicados em engenharia de tecidos, como a bioimpressão, abrindo ainda mais as possibilidades para pesquisa e potencialmente, aplicações clínicas.

Palavras-chave: organoides - bioimpressão 3D - cultura tridimensional - autoagregação - peptídeos ultracurtos - hidrogel - reologia - viabilidade celular - biomateriais - bioimpressão - engenharia de tecidos

Declaration

I hereby declare, under word of honor, that this work is original and that all non-original contributions is indicated, and due reference is given to the author and source.

Alexandra Antunes,

July 3rd 2023

Index

List of figures

List of tables

Notation and glossary

G'	Storage modulus	Pa
G''	Loss modulus	Pa
γ	Strain	$rad.s^{-1}$
	Luminescence	RLU

LIST OF ACRONYMS

ASCs	Adult stem cells
Calcein-AM	Calcein acetoxymethyl ester
DCM	Dichloromethane
ECM	Extracellular matrix
EthD-I	Ethidium homodimer-I
FBS	Fetal bovine serum
GBM	Glioblastoma
HEK293	Human embryonic kidney 293
HDFn	Human dermal fibroblasts neonatal
iPSCs	Induced pluripotent stem cells
MPSC	Multipotent stem cells
PBS	Phosphate-buffered saline
P/S	Penicillin/streptavidin
PFA	Paraformaldehyde
PSCs	Pluripotent cells
RT	Room temperature
SAP	Self-assembling peptides
TFA	Trifluoroacetic acid
PEP1	Peptide 1
PEP2	Peptide 2
PEP2-RGD	RGD functionalized peptide 2

1. Introduction

In recent years, there has been a need for improved *in vitro* models that can better replicate the complex architecture and physiological conditions of living tissues. Traditional two-dimensional (2D) cell cultures, while informative, do not accurately represent the intricate cellular microenvironment. They present limitations in cell-cell and cell-matrix interactions, a simplified morphology, and altered gene expression patterns. To address these limitations, the field of tissue engineering has witnessed a surge of interest in the development of biomaterial-based scaffolds capable of supporting three-dimensional (3D) cell culture systems. [1]

Among the promising biomaterials for 3D cellular model establishment, ultrashort self-assembling peptides (SAPs) have gained attention. These peptides, composed of mostly natural amino acids, possess unique characteristics that make them ideal scaffold materials. First, their composition ensures compatibility with living cells, minimizing any potential cytotoxic effects. Their properties are tunable: their biodegradability and anti-microbial effect can be controlled. Furthermore, the utilization of rationally designed peptides based on natural amino acids allows replication and reproducibility, essential factors for achieving standardization and scalability for diverse applications. [2]

Unlike many conventional biomaterials, SAP obviate the need for chemical or physical cross-linking agents, such as UV irradiation, to form stable hydrogels. This eliminates the requirement to subject cells to external factors that may disrupt their behavior or compromise viability. Instead, these peptides undergo self-assembly driven by inherent molecular interactions and forces, resulting in the formation of well-defined and structured matrices [3] This biomimetic characteristic closely emulates the extracellular matrix (ECM) present in natural tissues, creating an environment that facilitates cell interactions with their surroundings, particularly through focal adhesion points. These interactions are pivotal for cell signaling, proliferation, and differentiation processes, offering a more faithful representation of *in vivo* cellular behavior. Another advantage of SAP hydrogels over commonly used matrix materials, like Matrigel, is the absence of growth factors. While they play critical roles in cellular processes, their inclusion in culture systems introduces variability and complicates the interpretation of experimental results.

By eliminating the need for exogenous growth factors, peptide hydrogels provide a controlled and defined environment for investigating cellular behavior, enabling researchers to specifically study the influence of scaffold architecture and mechanical properties on cell function. [4]

The aim of this thesis is to evaluate the potential of SAPs as scaffolds for 3D organoid development. First, we will characterize the mechanical properties of four distinct peptide-based hydrogels and investigate their capacity to support cell viability and function across different cell types. Cell viability was assessed using live-dead assays, ATP assays, and cytoskeleton imaging techniques. Additionally, the suitability of the selected peptide hydrogels for bioprinting applications will be examined, to successfully fabricate cell-laden scaffolds.

The findings derived from this study will contribute to the expanding knowledge base surrounding biomaterials for 3D organoids establishment. Gaining insights into the mechanical properties and cell-interaction capabilities of these new can unlock novel outcomes for the development of advanced 3D cellular models

1. Context and state of the art

1.1. 3D organoids for *in vitro* research

1.1.1. 3D organoids

Organoids are 3D *in vitro* organ-like tissues aimed to mimic a specific *in vivo* organ. They are commonly generated from pluripotent stem cells or adult tissue stem cells via self-organization, resulting in the of organ-specific cell types. Human organoids are expected to mimic complex microenvironments and many of the *in vivo* structural and physiological functions of relevant tissues. The objective is to fill the translational gap between animals and humans to increase our understanding of diseases, developmental processes in studies of the organogenesis mechanisms, disease modelling, and screening of drug effects and/or toxicity. [5-8]

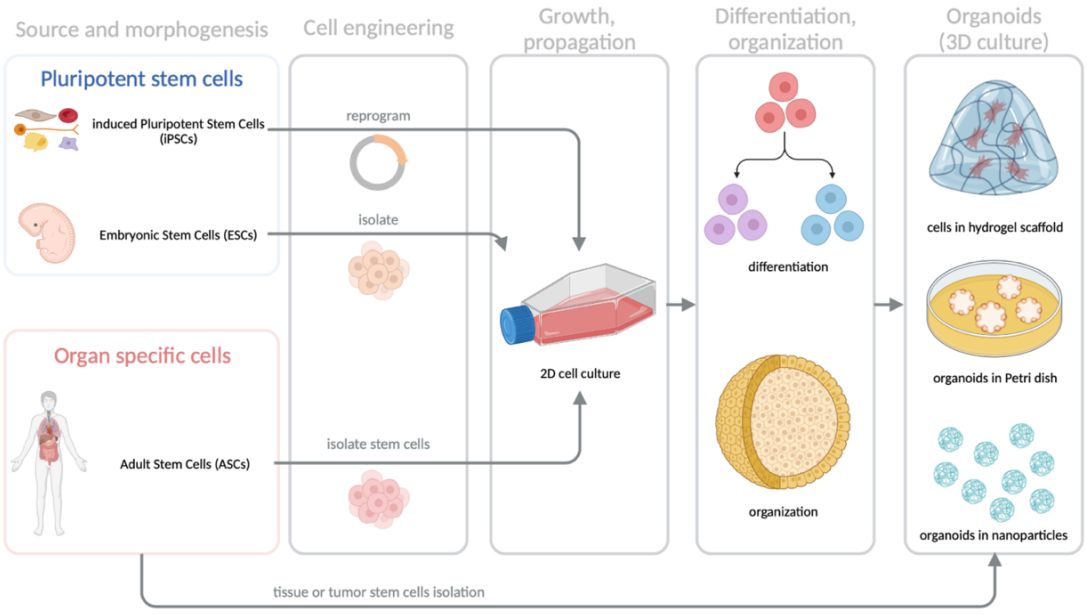

Figure 1. Schematic illustration of the organoid culture approach. Inspired by [6]. Created with BioRender.com

1.1.2. 3D organoids: applications

3D organoids have a variety of uses in different fields. In research, 3D organoids may be used to investigate human tissues and functions, to model and investigate diseases, their evolution and create regenerative medicines. In tissue biology, they enable extensive examination of stem cell morphogens, growth, and differentiation. In disease modeling,

organoids can be patient-derived for illnesses simulation like cancer, neurological disorders, infectious diseases. They serve as a support to study disease mechanisms / progression, identify potential therapeutic targets, test drug efficacy and toxicity and are a tool for personalized medicine development. By testing medications on patient-derived organoids, treatments are optimized for the patient and individualized therapeutics are generated, thus lowering adverse reactions risk and improving treatment outcomes. In regenerative medicine, patient / donor derived are genetically modified before transplant. [9-12]

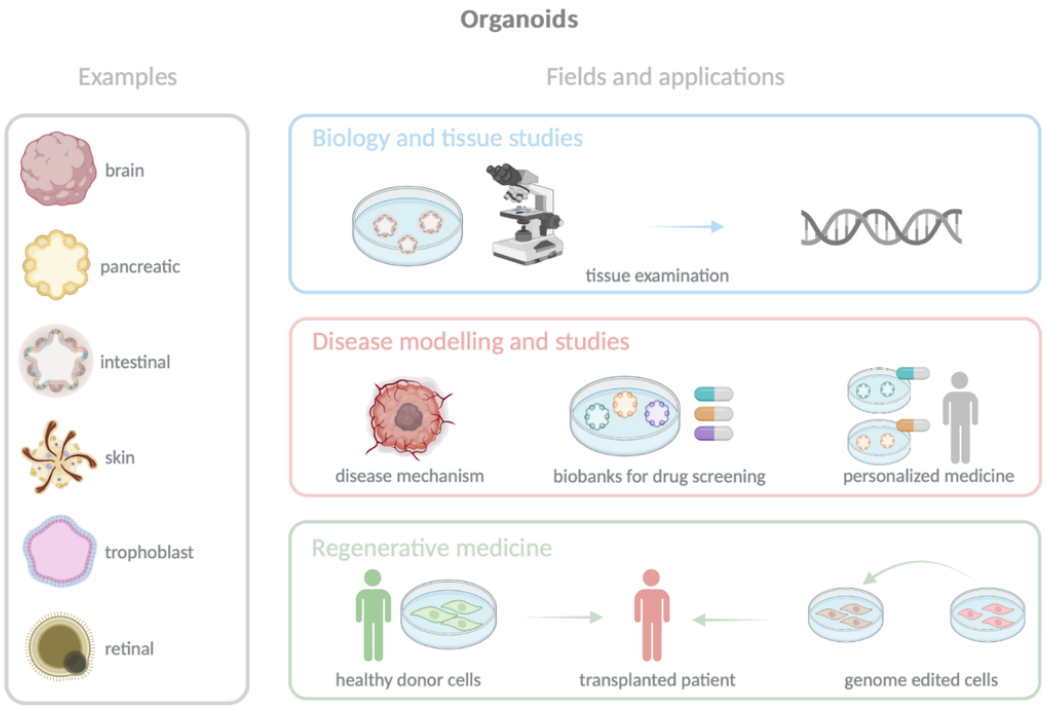

Figure 2. Organoids: examples of organoids and applications. Inspired by [12] . Created with BioRender.com

1.1.3. 3D organoids: advantages

3D organoids present numerous advantages compared to traditional methods. They can be derived from various types of stem cells, making them more versatile than traditional 2D cultures. They allow the cells to multidirectionally develop, to recreate the *in vivo* organogenesis and morphological features. Thus, the architecture and physiology of human organs is better simulated, providing a more accurate representation of biological systems. This provides a unique opportunity to complement animal models in research, for example to determine cell abnormalities causes. [9, 13]

1.2. Scaffold materials for 3D organoids development

1.2.1. Hydrogels: natural, synthetic, protein-engineered

Hydrogels used in 3D culture include natural, synthetic, and protein-engineered hydrogels that mimic the scaffolding support provided by the native extracellular matrix (ECM) of tissues. [14]

Reconstituted decellularized extracellular matrix (ECM) derived from natural sources, like the Engelbreth-Holm-Swarm (EHS) matrix (known as Matrigel, Geltrex, and Cultrex BME), have found use in the organoid field. However, they cause several issues. They contain growth-factor-binding proteins, leading to growth-factor sequestration and heterogeneous cellular response. Their mechanical properties are different than the ones from the ECM tissue (20-450 and 100-100,000 Pa respectively) and cannot be tuned. Batch-to-batch variations occur due to the complex proteins mixture. As this material comes from mouse tumor, it poses immunogenic and/or pathogenic reactions threat if transplanted. This makes the chemical characterization of the material impractical, hindering culture reproducibility and clinical translation. [14, 15] Natural biopolymers are also used to form single-component biopolymers matrixes and have shown promising results for organoid culture. They include protein-based matrices (collagen, polysaccharide-based materials like hyaluronic acid and alginate). They are chemically defined, thus allow for the control of material properties through chemical and physical modifications. Therefore, these materials exhibit less variability than EHS matrices, making them more robust for organoid culture. [14] Nonetheless, there are some drawbacks. Collagen needs extensive purification before cell seeding to make it less antigenic but may still transmit pathogens, causing immune reactions. Its poor mechanical properties difficult its fabrication and handling and allow less biodegradability control. Gelatin, (collagen derived) suffers from poor mechanical properties and needs extensive cross-linking (physical, chemical, or enzymatic) to be functional. Alginate presents a slow degradation rate that causes problems for tissue growth. Its weak mechanical integrity is an issue as a long-term cells scaffold. Hyaluronic acid present a limited range of mechanical properties for applications. [16]

Synthetic polymers allow countless possibilities in terms of material properties. Poly(ethylene glycol) (PEG) based hydrogels present numerous advantages. Those non-specific protein adsorbates prevent biofouling, are available in different structures and molecular weights, allow several matrices designs, can be functionalized (by bioligands, signaling molecules, crosslinking points integration) and are low-cost. Nonetheless, its non-specificity in protein adsorption makes data interpretation difficult. [14]

Protein-engineered hydrogels are composed by recombinant proteins, themselves inspired by native proteins. They can be functionalized to obtain defined and tunable properties from natural-protein biomaterials, including cell-adhesive domains. [14]

Hydrogel synthesis can be classified into two strategies: chemical synthesis and physical synthesis. Chemical synthesis involves the formation of covalent bonds through various cross-linking methods (enzymatic reactions, aldehyde reactions, condensation reactions, addition reactions, and free radical polymerization). Physical synthesis relies on intra- and intermolecular interactions driven by weak forces (hydrogen bonding, π-π stacking interactions, hydrophobic interactions, Van der Waals interactions, and crystallization). [17-19]

1.2.2. Ultrashort peptides scaffolds as a new material for organoid fabrication

Ultrashort peptides are a novel class of synthetic peptides that self-assemble at certain concentrations and under controlled physiological conditions to form a biomimetic hydrogel. They are amphiphilic molecules that spontaneously aggregate, forming 3D structures like nanofibers. The SAPs developed by the Hauser Group have demonstrated biocompatibility, biodegradability, and non-immunogenicity. Those rationally designed peptides present a better compositional control and consequently, a higher reproducibility compared to other materials. They find applicability in drug release, tissue engineering and 3D cell culture. [2, 20, 21]

1.2.3. Improving peptide scaffolds by biofunctionalization

Functionalization of ultrashort peptides can be achieved to improve their biocompatibility by enhancing certain properties: adhesion, migration, differentiation, mineralization etc. On ultrashort peptides, adding the fibronectin-derived peptide

sequence RGD or the collagen-derived peptide sequence GFOGER can improve their bioactivity and enhance their cell adhesion and proliferation properties. [14, 22-24]

1.3. Cell sources for 3D organoids development

Organoids can be derived from primary tissue or differentiated from pluripotent stem cells. They are classified in three groups: embryonic stem cells (ESCs), induced pluripotent stem cells (iPSCs), and adult stem cells (ASCs). [14, 25]

1.3.1. Multipotent stem cells (MPSCs)

ASCs are multipotent stem cells that are committed to a specific cell lineage, tissue and/or organ. The organoids derived from tissue-resident stem cells, progenitor cells, or differentiated cells from healthy or diseased tissues, (ex: tumors) can model specific organs (ex: gastrointestinal tract: esophagus, stomach, colon, and intestine, lung). Their specificity is essential for maintaining homeostasis of the adult tissues and form 3D organoid models that closely resemble their tissue of origin. [26]

1.3.2. Pluripotent Stem cells (PSCs)

Contrariwise, pluripotent cells (PSCs) can give rise to a broad set of cell types, according to the instructions they receive. Organoids derived from PSCs such as embryonic stem cells (ESCs) and induced pluripotent stem cells (iPSCs) can be reprogrammed to model a wide range of tissues and organs (brain, retina, intestine, kidney, liver). [9, 25-27]

1.4. Bioprinting for 3D organoids establishment

Several bioengineering strategies are associated to 3D organoids manufacturing. In this this work, low attachment cell culture plates, and bioprinting are used. Microfluidics were exploited as a side task.

1.4.1. Cell culture plates

Low attachment cell culture plates allow the growth of 3D organoids through cell-to-cell aggregation via naturally secreted extracellular matrices (ECM). The ECM are replicated within natural or artificial hydrogels. [25]

1.4.2. Bioprinting technology

Bioprinting is a digital manufacturing method using a 3D printer to reproduce organized tissue structures layer by layer. It relies on a 3D model created in CAD software. Bioprinted constructs can include various components: primary cells, ECM, cytokines, biomaterials (polymers, ceramics, or hydrogels). This technique allows for precise replication of complex tissue microenvironments and has been used to reproduce structures like vascular grafts, skin, bone, heart tissue, and cell scaffolds. [25, 28]

1.4.3. Microfluidics

Microfluidics technology is promising for advancing the development of 3D organoids. It allows for the creation of a microenvironment that closely resembles conditions in the body by continuous supply of nutrients and growth factors. With precise control over fluid flow and mixing, devices can replicate important feature: cell-cell interactions, matrix properties, biochemical/mechanical signals crucial for organoid development and function. Simple microfluidic 3D cell constructs can replicate a single cell type, while multicellular microfluidic devices, called organ-on-a-chip, enable complex structures with multiple cell types. These miniature devices and arrayed microfabrication techniques make microfluidics an appealing option for high-throughput studies on organoid development, disease modeling, and drug screening. [25]

1.5. Experimental tissues

1.5.1. Fibroblasts in connective tissues

HDF are essential cells found in connective tissues. They are vital in building and maintaining the surrounding tissue structure. Their elongated, spindle-shaped morphology readily attaches and moves across tissue culture substrates. Their function is to build, maintain, and alter connective tissue stromas that functionally interact with other tissues such as epithelial tissues from embryonic development to aging. They can be found in nearly every tissue and organ. Their functional definition can be broadened by describing a population of cells that synthesize and secrete a complex array of structural and nonstructural matricellular family of molecules, respectively collagens, fibronectin and thrombospondins, osteopontin. These ECM molecules actively organize and redefine

by producing proteinases, and communicate with adjacent cells via paracrine, autocrine, and other means. Their contribution to tissue aging and, participate directly or indirectly in fibrotic illnesses and nonhealing wounds. [29]

1.5.2. Human embryonic kidney 293 cells

Human embryonic kidney 293 (HEK293) are immortalized cells, which stem from primary human embryonic kidney cells, are one of the most used host cells of human cell lines. They are characterized by a high transfection efficiency using the most common transfection reagents with large quantities of recombinant proteins produced. They represent an ideal host cell for large-scale suspension cultures in pharmaceutical manufacturing. Their potential for high growth rate and cell density in shake flasks, efficient and flexible metabolism, and easy genetic manipulation gives them advantages as biotherapeutics production tools. Their human-like posttranslational modifications abilities enables them to produce proteins similar to those naturally synthesized in humans. Their sensitivity makes them more susceptible to environmental factors *in vitro*, thus they make a suitable model for new drug discovery and toxicity testing. Therefore, their use is widely spread to produce recombinant therapeutic proteins, vaccines, anticancer agents, and other clinically relevant drugs. [30]

1.5.3. Glioblastoma SH-SY5: a brain tumor

Glioblastoma (GBM), the most common primary brain tumor is one of the hardest malignancies to treat. [31] Improvements have been made, but results are typically not encouraging; patients usually suffer from an uncertain future. [32] Its cellular diversity and heterogeneous microenvironments make treatment challenging. Microscopically, GBM is heterogeneous with a high degree of cellularity, nuclear atypia, cellular pleomorphism, mitotic activity, microvascular proliferation and necrosis. [33]

3D organoid cultures have previously shown potential as a platform that provides a better insight of the complex network of interactions of glioblastoma to help better understand GBM. [31]

The neuroblastoma SH-SY5Y cell line is a subline of the SK-N-SH cell line, which was established in culture in 1970 from a bone marrow biopsy of a 4-year-old female's metastatic neuroblastoma and has gone through three rounds of clonal selection. [34]

3. Materials and methods

3.1. Ultrashort peptides-based hydrogels preparation

3.1.1. The tetrameric ultrashort self-assembling peptides: IIZK, PEP1, PEP2, PEP2-RGD

The rationally designed peptides that were investigated are listed in Table 1.

Table 1. List of the peptides investigated (IIZK, PEP1, PEP2, PEP2-RGD), molar masses and functionalization.

Peptide sequence	Molecular weight (g/mol)	Functionalisation
IIZK	566.78	none
PEP1	566.78	none
PEP2	566.78	none
PEP2-RGD	1153.33	RGD sequence (cell attachement)

3.1.2. Solid phase peptides synthesis

The reactants 9-fluorenymethoxycarbonyl (Fmoc)-protected amino acids, MBHA rink amide resin beads (0,669 moles of linker per gram of beads), TBTU, and hydroxy benzotriazole (HOBt) were obtained from GL Biochem in Shangai, China. Sigma-Aldrich provided N,N-diisopropylethylamine (DIPEA), piperidine, acetic anhydride, trifluoroacetic acid (TFA), triisopropylsilane, N,N-dimethylformamide (DMF), dichloromethane (DCM), diethyl ether, and ethanol. The ultrashort peptides IIZK, PEP1, PEP2and PEP2-RGD were synthesized by Fmoc-based solid-phase peptide synthesis process (SPPS) and purified by reverse-phase HPLC. Before coupling the first amino acid, the Fmoc group on resin was deprotected using 20% (v/v) piperidine/DMF. Amino acid coupling was carried out by adding TBTU (3 equiv), HOBt (3 equiv), DIPEA (6 equiv), and Fmoc-protected amino acid (3 equiv) to the reaction vessel and agitating it for 90 minutes. The Kaiser test was carried out at the end of the coupling process to certify that the coupling reaction had been completed. The N-terminus of the peptide was acetylated with a combination of 2:6:1 (v/v) acetic anhydride:DIPEA:DMF. Finally, a 95:2.5:2.5 mixture of TFA, water, and triisopropylsilane was added to cleave the peptide from the resin. The peptide was then dispersed in cold diethyl ether and left to stand overnight at 4 °C. The peptide was then

centrifuged and dried in a vacuum desiccator. The peptides were subsequently purified in reversed-phase prep HPLC using a C-18 column. According to HPLC data, the purity of the peptides IVFK and IVZK was greater than 96%. After lyophilization, both pure peptides were collected with greater than 60% yield.

3.1.3. Hydrogel formation

For the gelation test, 1 mL peptide solutions were prepared by dissolving lyophilized peptide powders, previously left at room temperature (RT) for 15 min. They were dissolved in 900μL of MilliQ water and vortexed until fully dissolved. The hydrogel formation was initiated by adding 100μL (10% of the total volume) of 10X phosphate-buffered saline (PBS) to the solution.

3.2. Hydrogel physical and chemical characterization

3.2.1. Critical gelation concentration determination

Vial inversion tests were performed to each peptide using different concentrations. The tested concentrations are presented in Table 2.

After the PBS addition to the vials, the chronometer was started, and the hydrogel state checked visually every minute until solid to determine the critical gelation concentration.

Table 2. Minimum gelation concentration determination. Peptides and concentrations for inverted vial test.

Peptide / Sample n°	Sample concentration ($mg.mL^{-1}$)				
	Control	1	2	3	4
IIZK	2.00				
PEP1		1.00	2.00		
PEP2		1.00	1.50	2.00	
PEP2-RGD		1.00	2.00	3.00	10.00
PEP2/ PEP2-RGD (1:1)		2.00	3.00	5.00	
PEP2/ PEP2-RGD (2:1)		2.00	3.00	5.00	
PEP2/ PEP2-RGD (5:1)		2.00	3.00	5.00	

3.2.2. Rheology assay

The mechanical stiffness of the peptide hydrogels was analyzed by rheometry. The rheometer used is the TA Ares-G2 Rheometer. It is equipped with parallel-plate geometries of 8 mm diameter. The experiment was performed at RT. The sample gap between the upper and the lower geometries was set individually for each sample. The hydrogels were prepared from 135 µL of peptide solution, mixed with 15 µL of 10X PBS in an 8 mm poly(methyl methacrylate) (PMMA) casting ring and left for 12 hours at RT before measurement. The rings were kept inside tightly sealed Petri dishes at RT and surrounded with water to avoid dehydration. To control the accuracy of the measurements, six replicates for each peptide hydrogel concentration were prepared. The stiffness was analyzed through three successive tests, which were time sweep, frequency sweep, and amplitude sweep. Time sweep was first performed for 5 min with an angular frequency and a strain of 1 rad/s and 0.1%, respectively. A frequency sweep was subsequently performed on the sample for a range of angular frequency of 100−0.1 rad/s with the same strain of 0.1%. The tests were completed with the amplitude sweep by applying a gradual increase of strain from 0.01% to 100% at 1 rad/s angular frequency.

3.3. Cell culture and expansion

3.3.1. Fibroblasts: cell sources and expansion

Human dermal fibroblasts neonatal (HDFn) were purchased from Thermo Fisher Scientific, USA. Cells suspensions were used after 9 and 11 passages. The growth medium was prepared with 500 mL of Dulbecco's modified eagle medium (DMEM, ×1) supplemented with 10% fetal bovine serum (FBS), and 1% penicillin/streptavidin (P/S). The cells were added to 50 mL of growth medium. The mixture was centrifuged at 250 rpm for 5 min at RT to separate the cells, in the pellet from the DMSO storage buffer and the media, in the supernatant. Then, cells were resuspended in 25 mL of growth medium within cell-treated flasks and incubated for 7 days at 37°C under 5% CO_2. After incubation, the cells were viewed under a microscope to determine their confluency. The culture medium was renewed every 3 days.

After 7 days, the growth medium was removed, and the flasks washed with PBS (1X). 5 mL of 0.05% trypsin-ethylenediaminetetraacetic acid (×1) were added in each flask to detach them from the surface. The flask was then incubated at 37°C for 5 min. After the incubation period, the cells were examined under an optical microscope to confirm detachment. Finally, the solution was transferred into a clean 50-mL centrifuge tube with 10-mL of fresh DMEM (×1) to inactivate the trypsin. Then, the cell suspension was centrifuged as described before, and the supernatant was discarded. Then, the cell pellet were transferred to 50 mL tubes and media was added.

3.3.2. Human embryonic kidney 293: cell sources and expansion

Human embryonic kidney 293 (HEK293) cells were purchased from Thermo Fisher Scientific, USA. Cells suspensions were used after 9 and 10 passages. The same growth medium was used. The cells were added to 50 mL of growth medium. They were incubated in the same conditions. The following steps are described in section 3.3.1

3.3.3. Glioblastoma: cell sources and expansion

Glioblastoma (GBM) SH-SY5 cells were purchased from Thermo Fisher Scientific, USA. Cells suspensions were used after 10 and 11 passages. The same growth medium was used. Cells were resuspended in 13 mL of growth medium. They were incubated in the same conditions. The following steps are described in section 3.3.1

3.4. 3D cultures: Cell seeding and growth

3.4.1. Hydrogel scaffold preparation

First, the peptides were weighted and sterilized under UV light for 30 min for sterility. The peptides were then mixed with 1mL of sterile distilled water under sterile conditions and vortexed. 96-well plates were used to form the 3D layers of hydrogel. For each well, 20 µL the peptide solution and 20µL of 2X PBS were mixed to form the hydrogel scaffold. The peptides concentrations used for 3D culture are presented in Table 3.

Table 3. Peptide concentrations in the 3D hydrogel and hydrogel pre-solution.

Peptide	Ratio	Peptide concentration in plated hydrogel ($mg.mL^{-1}$)	Peptide concentration in initial solution ($mg.mL^{-1}$)
IIZK	-	2.00	4.00
PEP1	-	2.00	4.00
PEP2	-	2.00	4.00
PEP2/ PEP2-RGD	2:1	3.00	6.00
PEP2/ PEP2-RGD	5:1	2.00	4.00

For each type of cells, 3 plates were prepared for observation on day 1, day 3 and day 7, each for 3 different types of assays: ATP assay (6 replicates/peptide/plate), live/dead assay (3 replicates/peptide/plate) and immunostaining assay (3 replicates/peptide/plate).

3.4.2. Cells seeding

For the ATP assay, 2000 cells were seeded per well. 10000 cells per well were seeded for other assays. The cells were previously suspended in fresh growth medium prepared with 500 mL of Dulbecco's modified eagle medium (DMEM, ×1) supplemented with 10% fetal bovine serum (FBS), and 1% penicillin/streptavidin (P/S).

3.4.3. Cells growth

Cells were maintained in a fresh growth medium and incubated at 37°C at 5% CO_2. The culture media was changed every 3 days. Cells were split using trypsin and then mixed with media before loading onto the hydrogel layers.

3.5. Biocompatibility and morphological assessment

3.5.1. ATP assay

The CellTiter-Glo® luminescent 3D cell viability assay was used to observe the proliferation rate of cells in 3D peptide cultures. The reactant induces cell lysis to produce a bioluminescent signal proportional to the amount of ATP present (or metabolically active cells).

For each well, 100 µL of media was replaced by 100 µL of CellTiter-Glo®. The mixture was vigorously mixed to dismantle the hydrogel and allow the in-scaffold cells to contact

with the reactant, followed by an incubation period of 25 min at RT. The bioluminescent signals were read using a plate reader (PHERAstar FS, Germany). The metabolic activity of the cells was evaluated after 1, 3 and 7 days.

3.5.1. Live / dead assay

The viability of the cellular 3D constructs was examined using the Live/Dead Viability/Cytotoxicity Kit (Invitrogen, ThermoFisher, USA). Calcein acetoxymethyl ester (Calcein-AM) was used as a marker for living cells and ethidium homodimer-I (EthD-I) for dead cells. The staining solution was prepared by mixing 2 µL of Calcein-AM and 4 µL of EthD-I in 1mL of 1X PBS. The solution was added to the wells and incubated for 30 min at RT. After the incubation period, stained cells were imaged with an EVOS M7000 microscope (Invitrogen, ThermoFisher, USA). The viability of the cells was assessed after 1, 3 and 7 days.

3.5.2. Cytoskeletal staining

Immunostaining was performed using Rhodamine phalloidin (Invitrogen, Thermo Fisher) for F-actin staining. The cells were first fixed with 4% paraformaldehyde (PFA) for 30 min and washed and covered with 1X PBS before being stored at 4ºC. They were then permeabilized with cytoskeletal buffer (0.5% Triton X-100, 300 mM sucrose, 3 mM MgCl2 in 25 mL of 1X PBS) for 5min at RT. The permeabilized cells were then washed (1X PBS) and incubated in a blocking buffer solution (5% FBS, 0.1% Tween 20, 0.02% Sodium Azide in 100mL of 1X PBS) for 30 min at RT. Rhodamine phalloidin (1:40 in 1X PBS) was added to the cells and left for 1h at RT. Thereafter, the cells were washed with 1X PBS and incubated in DAPI (1:1500 water) for 10 min at RT to stain the nucleus. Fluorescence confocal microscopy (Zeiss LSM 710 Inverted Confocal Microscope, Germany) was used to observe the cell morphology.

3.6. Fabrication of the 3D-printed ultrashort peptides scaffold

3.6.1. Extrusion-based 3D printing of ultrashort peptides scaffolds

The robotic 3D printing system consists of three microfluidic pumps (ExiGo by Cellix), a 4-axis robotic arm (DOBOT Magician by DOBOT), and a dual-coaxial nozzle previously

engineered in the laboratory. Each microfluidic pump was attributed to one solution: one for the peptide solution, one for the Phosphate-Buffered Saline (PBS), and the other for the cell suspension (or 1X PBS for acellular prints). The pumps system enables the control of the flow rates for each individual pump. A modified head previously printed in the laboratory was used to mount the nozzle. The nozzle design includes three inlets for the solutions and one outlet with a 0.5 mm inner diameter. Two of the inlets are used to form the ink by mixing the peptide solution and PBS to form the hydrogel, and the third is for cell dispensing. Peptide flow rates were previously optimized for each peptide solution. Flowrates of 15 µL/min were used for the PBS and the cell suspension. The printing files were designed with SOLIDWORKS and transferred to Repetier-Host to obtain the G-code for 3D printing with the robotic arm.

3.6.2. Determination and optimization of the 3D-printing parameters

To determine the initial printing parameters, optimization experiments were run with the 3D printing system. Gelation time, printability, stiffness, clogging and resolution were qualitatively evaluated with the aim of reaching the best results at a minimal peptide concentration. The parameters are presented in Table 4.

Table 4. Parameters for optimal initial printing parameters establishment

Peptide	Concentration ($mg.mL^{-1}$)	PBS	Pump flows (µL/min)			Gelation time (s)	Observations		
			Pump 1 (peptide)	Pump 2 (PBS)	Pump 3 (1X PBS)		Stiffness	Clogging	Resolution
IIZK	13	7X	50.00	15.00	15.00	00:00:30			
IIZK	13	5X	45.00	15.00	15.00	00:00:35			
IIZK	**10**	**5X**	**50.00**	**15.00**	**15.00**	**00:00:45**			
IIZK	10	5X	45.00	15.00	15.00	00:01:00			
IIZK	8	5X	50.00	15.00	15.00	00:01:30			

3.7. Evaluation of the peptide influence in the printing

3.7.1. Gelation time in the nozzle

Before starting the printing, the gelation time of each peptide was evaluated. The aim is to adjust the concentration in order to get closer to the value that allowed a smooth printing process with the control IIZK, while targeting the lowest concentration possible in

the 3D construct to ensure a higher cell viability for the bioprinting. The targeted values are presented and bolded in Table 4. Basal flow rates of 50/15/15 µL/min were used for the peptide solution, 5X PBS and 1X PBS respectively, for further optimization.

3.7.2. Regularity, continuity and resolution of the printing

To evaluate the regularity and continuity of the printing, a 2 layers square spiral (2x2 cm) and a 20 layers cylinder (∅ 2cm) were 3D printed. Based on the optimized parameters obtained for the gelation time, the flow rates were set for each peptide. The regularity and continuity of the constructs were evaluated by observing the formation of the thread at the nozzle tip and the layer deposition.

The resolution and the shape fidelity were evaluated by comparing the printings dimensions and definition with the CAD files specifications.

3.8. 3D bioprinted organoids: cell culture and growth

3.8.1. 3D bioprinting process

The same printing system was used for bioprinting. The nozzles and tubes were flushed with ethanol (x2) and MilliQ water (x3) for sterility. The material (printer, nozzle, slides, petri dished, twizzers etc.) and the weighted peptide powders were sterilized under UV light for 30min. The peptides were then diluted in 1mL of sterile water, vortexed and sonicated until homogeneous. Pumps 1 and 2 were loaded with peptide solution and 5X PBS respectively. Pump 3 was loaded with the cell suspension. The previously determined optimal flow rates of for each peptide min were used for the bioprinting.

3.8.2. Cell culture and growth in 3D-printed scaffolds

3D structures were bioprinted on glass slides in Petri dishes. The maintenance is described in Section 3.4.3.

Note: In all the experiments, IIZK was used as a control. For cellular activity experiments realized in 96-well plates, 2D was also used as a control.

4. Results and discussion

4.1. Mechanical properties of the SAPs hydrogels

4.1.1. Minimum gelation concentration of SAPs solutions

The gelation test results (Appendix 1) confirmed that IIZK has a minimum gelation concentration (MGC) of 2 $mg.mL^{-1}$, PEP1 similarly showed an MGC of 2 $mg.mL^{-1}$, PEP2showed an MGC of 1.5 $mg.mL^{-1}$. PEP2-RGD didn't gel at on its own but when mixed with PEP2at a ratio PEP2:PEP2-RGD (1:1) clumps started to form for concentrations of 3 $mg.mL^{-1}$ and 5 $mg.mL^{-1}$ at minutes 5 and 4 respectively. Using a ratio of 2:1, the MGC was established at 3 $mg.mL^{-1}$ with the obtention of a hydrogel at minute 2. For a ratio of 5:1, the MGC was also established at 3 $mg.mL^{-1}$ with the obtention of a hydrogel in the first minute. The results of the inverted vial test are summarized in Table 5.

Table 5. Minimum gelation concentrations of the ultrashort peptides (IIZK: control; PEP1; PEP2; PEP2-RGD; PEP2/PEP2-RGD 1:1; PEP2/PEP2-RGD 2:1; PEP2/PEP2-RGD 5:1).

Peptide	Ratio	Minimum gelation concentration (mg.mL-1)
IIZK	-	2.00
PEP1	-	2.00
PEP2	-	1.50
PEP2-RGD	-	-
PEP2/ PEP2-RGD	1:1	-
PEP2/ PEP2-RGD	2:1	3.00
PEP2/ PEP2-RGD	5:1	2.00

The MGC cited in Table 5 are the ones used in the experiments of hydrogel cell seeding except for the ratio (1:1) and PEP2which will be seeded at a concentration of 2 $mg.mL^{-1}$ for results uniformity.

4.1.2. Rheological properties of SAPs hydrogels

The rheological properties of the peptide hydrogels were analyzed through the storage modulus *G'* and loss modulus *G''*(Pa) in an oscillatory rheology frequency sweep. The frequency range for the experiment was 0.1 – 100 $rad.s^{-1}$.

Frequency sweep

The frequency sweep is used to characterize the stiffness, elasticity, and viscosity of a material. *G'* provides information about the material's ability to recover its shape after

deformation. G'' reflects its heat dissipation capacity and viscous behaviour. The frequency dependency reveals distinct regions associated with those behaviours. The results are presented in Figure 3, Figure 4, Figure 5, Figure 6 and Figure 7.

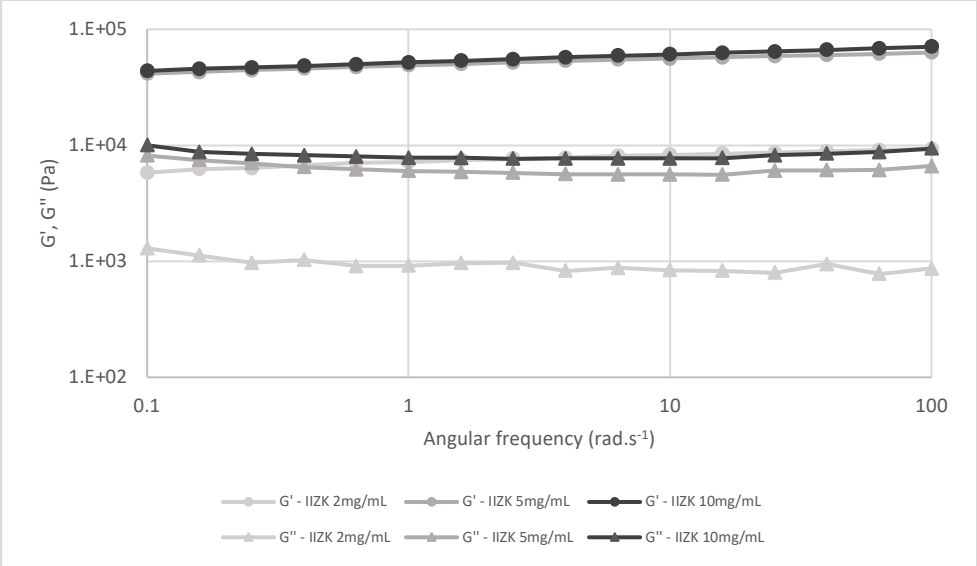

Figure 3. Rheological characterization. Frequency sweep of IIZK at 2mg.mL^{-1} , 5mg^{-1} and 10mg.mL^{-1} .

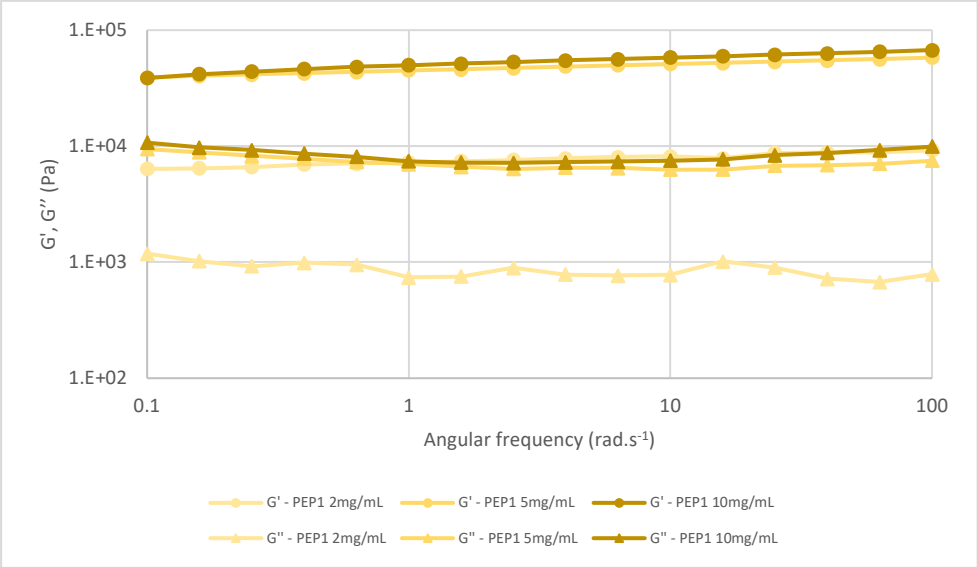

Figure 4. Rheological characterization. Frequency sweep of PEP1 at 2mg.mL^{-1} , 5mg.mL^{-1} and 10mg.mL^{-1} .

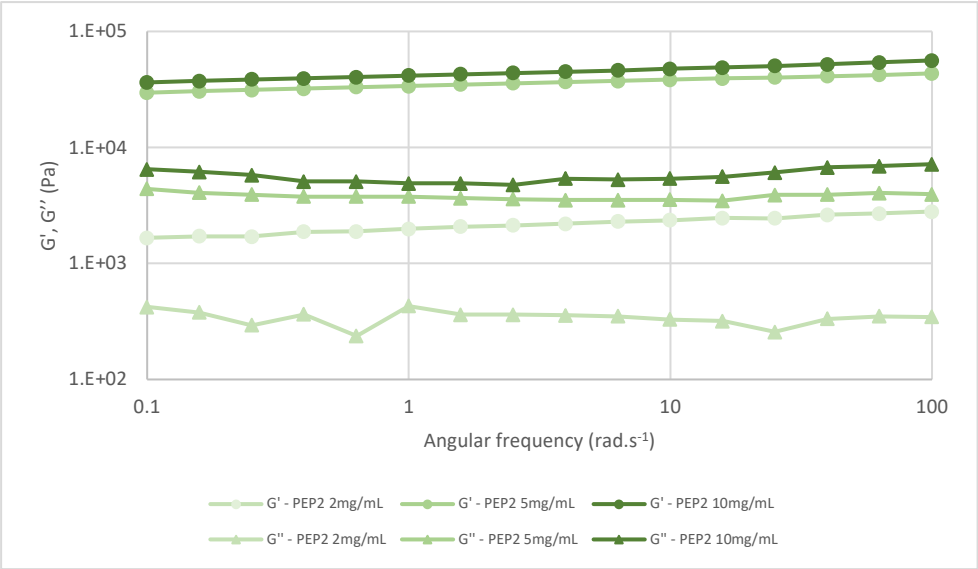

Figure 5. Rheological characterization. Frequency sweep of PEP2at 2mg.mL^{-1} , 5mg.mL^{-1} and 10mg.mL^{-1} .

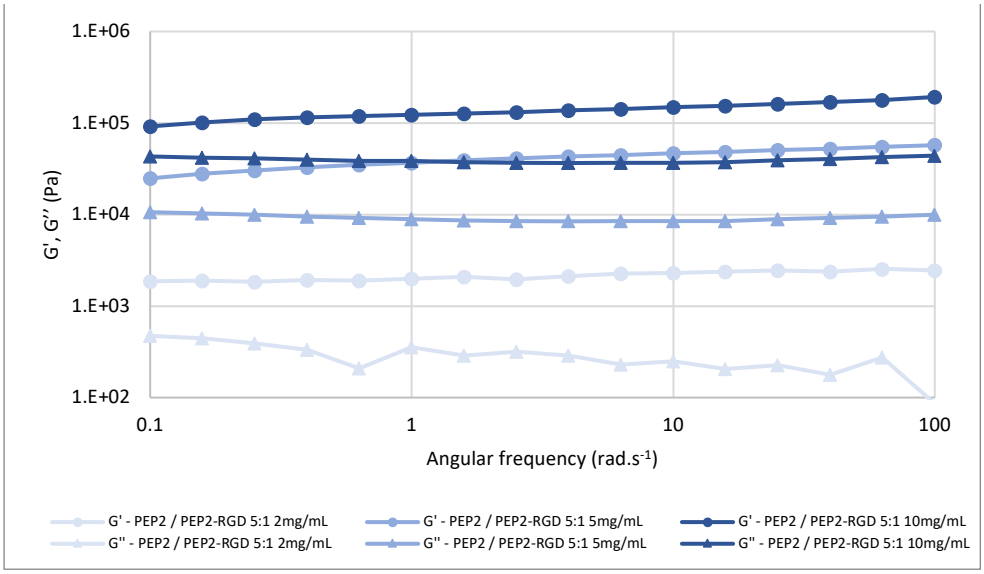

Figure 6. Rheological characterization. Frequency sweep of PEP2/PEP2-RGD (5:1) at 2mg.mL^{-1} , 5mg.mL^{-1} and 10mg.mL^{-1} .

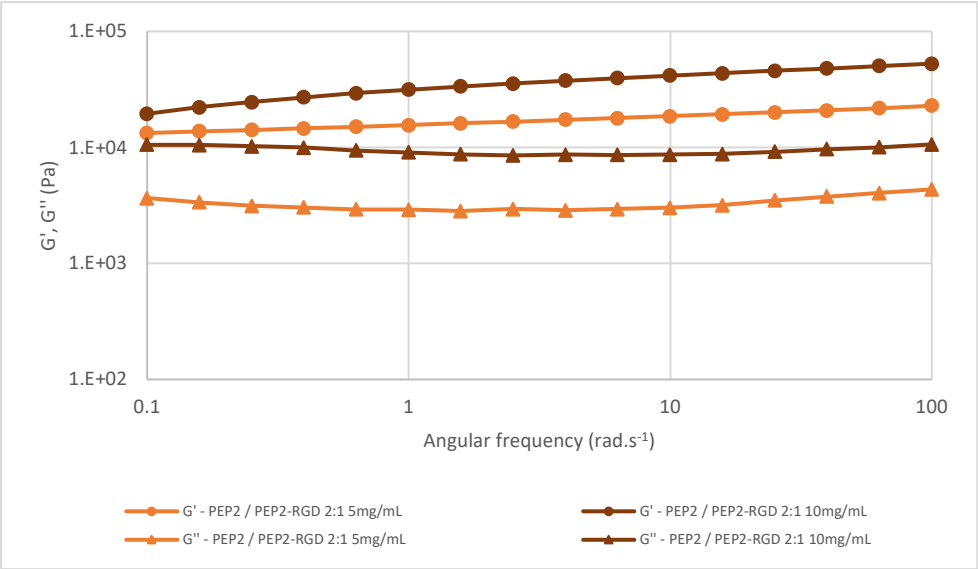

Figure 7. Rheological characterization. Frequency sweep of PEP2/PEP2-RGD (2:1) at 2mg.mL^{-1} , 5mg.mL^{-1} and 10mg.mL^{-1}

.

All peptides (PEP1, PEP2, PEP2/ PEP2-RGD (5:1), PEP2/ PEP2-RGD (2:1)) exhibit elastic behavior similar to the control. *G'* values increase with peptide concentration, indicating higher stiffness and energy storage.

G'' values increase with peptide concentration, indicating higher viscosity and energy dissipation. However, *G''* values remain relatively low for all peptides, indicating a predominant elastic behavior. PEP2/ PEP2-RGD (5:1) at the highest concentration shows the highest *G''* values, indicating the highest viscosity.

Peptide concentration affects stiffness levels. IIZK, PEP1, and PEP2show similar trends with increasing concentration, resulting in higher stiffness. PEP2/ PEP2-RGD (5:1) and (2:1) exhibit different stiffnesses than PEP2, which indicates that the functionalized peptide has an influence on the stiffness, which is non-linear.

In summary, PEP1 and PEP2hydrogels show comparable behaviors compared to the control IIZK in terms of elasticity, viscosity, and stiffness. PEP2-based hydrogel maintains similar behavior with less elasticity. PEP2/ PEP2-RGD (5:1) hydrogel exhibits higher stiffness at the highest concentration compared to the control, while its behavior at lower concentrations differs. The RGD functionalization has a non-linear influence on the stiffness.

Amplitude sweep

The amplitude sweep (or strain sweep) is used to analyze the viscoelastic properties of materials while varying the applied strain (γ). It is aimed to determine the length of the linear viscoelastic region (LVR). For all the hydrogels tested, the LVR is characterized by a strain amplitude-independent modulus at low strains. However, once the applied strain surpasses a critical value (γc), the behavior becomes nonlinear. Thus, the modulus magnitude starts to decrease, marking the end of the LVR. The results are presented in Figure 8.

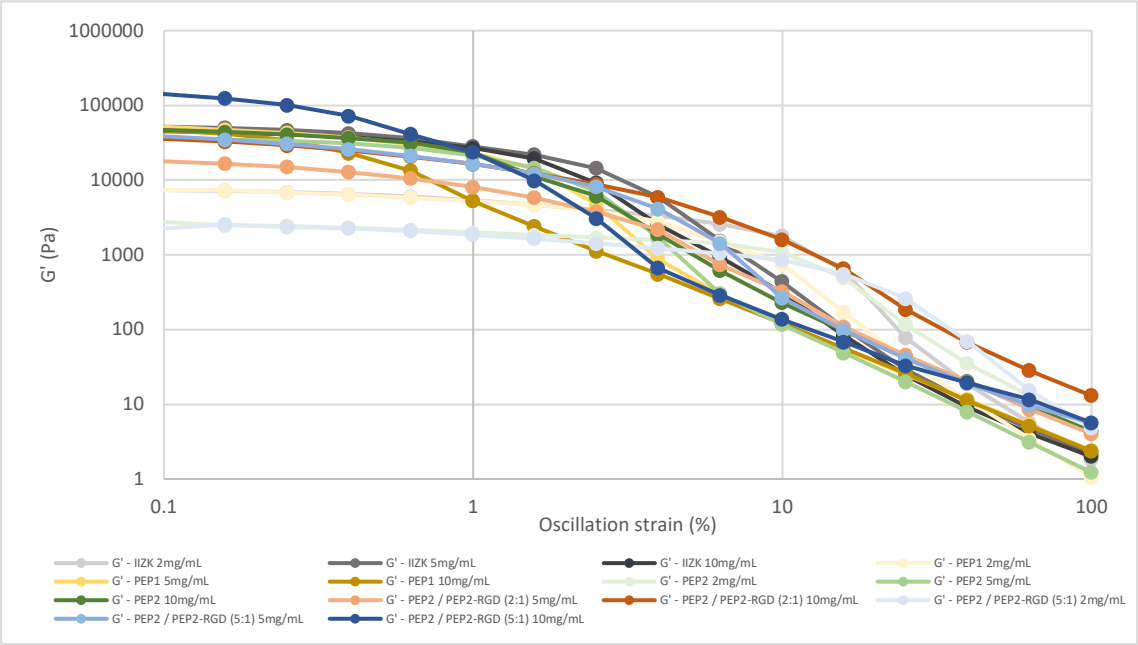

Figure 8. Rheological characterization. G'(Pa) vs Oscillation strain (%) Amplitude sweep of tested peptides at 2mg.mL^{-1}, 5mg.mL^{-1} and 10mg.mL^{-1}.

IIZK demonstrates a shorter linear viscoelastic region (LVR) at higher concentrations. This suggests that IIZK exhibits a higher level of elasticity at lower concentrations.

PEP1 exhibits a shorter LVR region compared to the control, indicating lower overall elasticity. At the lowest concentration, PEP2shows *G'* values that closely align with those of IIZK, suggesting a similar LVR region and elasticity. This indicates that PEP2shares similar elastic properties with IIZK at low concentrations. At the medium concentration, PEP2exhibits results more in line with PEP1, indicated by a shorter LVR compared to IIZK.

This suggests that the elasticity of PEP2decreases and becomes closer to PEP1 as the concentration increases.

At the highest concentration, the *G'* values of PEP2follow the trend observed in the control hydrogel, but with a slightly shorter LVR. This implies that PEP2approaches the elasticity of the control at high concentrations but still retains a slightly lower elasticity.

The (5:1) ratio of PEP2/ PEP2-RGD exhibits a similar LVR compared to IIZK and PEP2at 2 $mg.mL^{-1}$, indicating comparable elastic properties at this concentration. At 5 $mg.mL^{-1}$, the (5:1) ratio falls between the elastic properties of IIZK and PEP2. This suggests that the addition of RGD in this ratio affects the elasticity and results in intermediate properties.

At the highest concentration of 10 $mg.mL^{-1}$, the (5:1) ratio displays the shortest LVR among all the peptides, indicating the lowest elasticity. This indicates that the presence of RGD in this ratio significantly affects the elasticity, leading to decreased elasticity compared to other peptides. The (2:1) ratio of PEP2/ PEP2-RGD shows similar tendencies as IIZK at 5 $mg.mL^{-1}$, indicating a similar LVR and elasticity at this concentration. At 10 $mg.mL^{-1}$, the LVR of the (2:1) ratio is the longest among all peptides, presenting the highest elasticity. This suggests that the (2:1) ratio can form a more elastic network at higher concentrations compared to other peptides.

In summary, the comparison of the peptides characteristics reveals that IIZK demonstrates better elasticity at lower concentrations. Both PEP1 and PEP2display lower overall elasticity with shorter LVR regions compared to IIZK. The addition of RGD in the PEP2/ PEP2-RGD ratios (5:1) and (2:1) affects the elasticity, with the (5:1) ratio showing lower elasticity and the (2:1) ratio demonstrating higher elasticity compared to other peptides. This correlates with the previous results.

Time sweep

The results are completed by the analysis of the time sweep experiment, Figure 9.

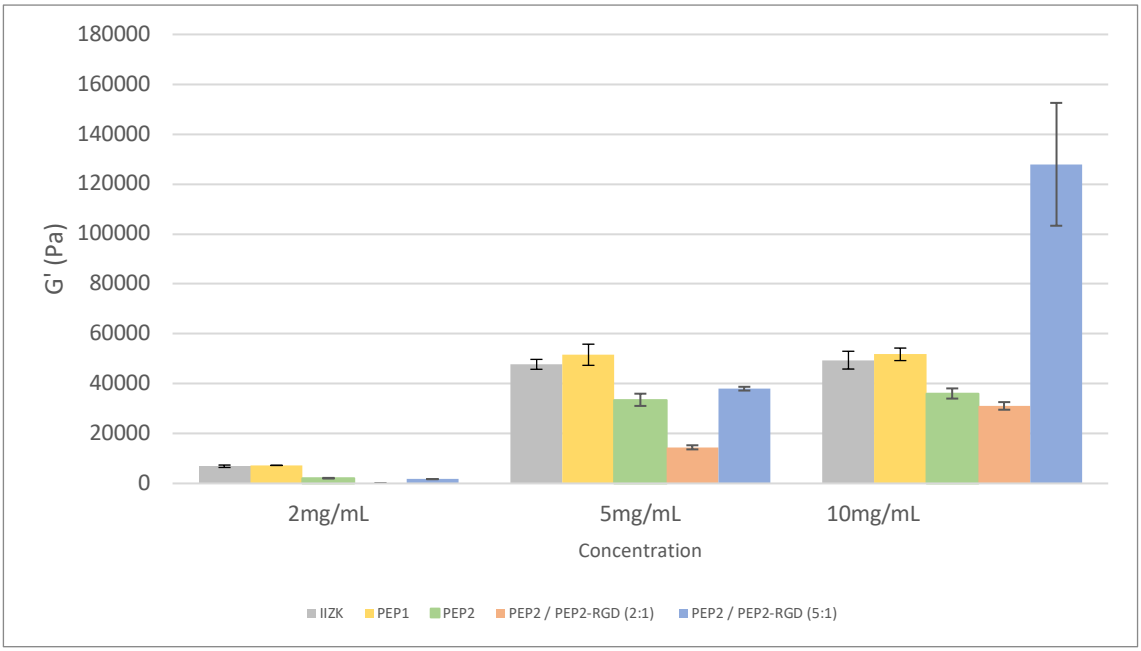

Figure 9. Rheological characterization. G'(Pa) vs Concentration (mg.mL^{-1}). Time sweep of tested peptides at 2mg.mL^{-1} , 5mg.mL^{-1} and 10mg.mL-1 .

At the lowest concentration of 2 mg.mL^{-1}, the control hydrogel exhibits a storage modulus of 6.9 kPa. PEP1 presents a slightly higher storage modulus than the control, suggesting it is similar in stiffness to IIZK. PEP2and PEP2-RGD (5:1) show very low storage moduli, indicating a weak network with low intermolecular interactions, thus a low stiffness. The ratio PEP2-RGD (2:1) was in a liquid state after 12h of preparation, so data could not be retrieved. Therefore, its stiffness characteristics cannot be determined. However, the liquid state suggests low stiffness.

At 5 mg.mL^{-1}, the control hydrogel exhibits a storage modulus of 48 kPa, indicating a higher stiffness compared to the lowest concentration. The difference in stiffness between PEP1 and IIZK increases, suggesting that PEP1 becomes softer than IIZK. The other peptides (PEP2, PEP2-RGD (5:1), and PEP2-RGD (2:1)) present lower stiffnesses than the control. Among them, PEP2/ PEP2-RGD (5:1) is stiffer than PEP2but softer than IIZK. PEP2/ PEP2-RGD (2:1) is the softest among the tested peptides, with a storage modulus of 14 kPa.

At 10 mg.mL^{-1}, the control , PEP1, and PEP2present similar *G'* values similar to the concentration of 5 mg.mL^{-1}, indicating consistent stiffness within this range. PEP2/ PEP2-RGD (2:1) exhibits a *G'* value similar to PEP2, suggesting a comparable stiffness . PEP2/

PEP2-RGD (5:1) shows a tremendous increase in stiffness, reaching a *G'* equal to 128 kPa, significantly higher than the other peptides.

In summary, PEP1 is similar to IIZK in terms of stiffness at low concentrations. For intermediate concentrations, PEP2and PEP2-RGD (5:1) exhibit lower stiffnesses than the control. PEP2-RGD (5:1) is stiffer than PEP2but softer than IIZK. PEP2-RGD (2:1) demonstrates the softest behavior among the peptides. The addition of RGD in the PEP2/ PEP2-RGD ratios (5:1) and (2:1) leads to distinct stiffness profiles, with the (5:1) ratio displaying a significant increase in stiffness compared to other peptides at high concentrations.

4.2. Influence of the peptides on cells activity

4.2.1. Cells viability analysis by live/dead assay

The biocompatibility and cytotoxicity of the peptides were analyzed qualitatively using live/dead staining. The green color indicates a cell viability, the red color indicates dead cells. The imaging results are presented in Figure 10, Figure 11 and Figure 12.

Peptide	Day 1	Day 3	Day 7
2D	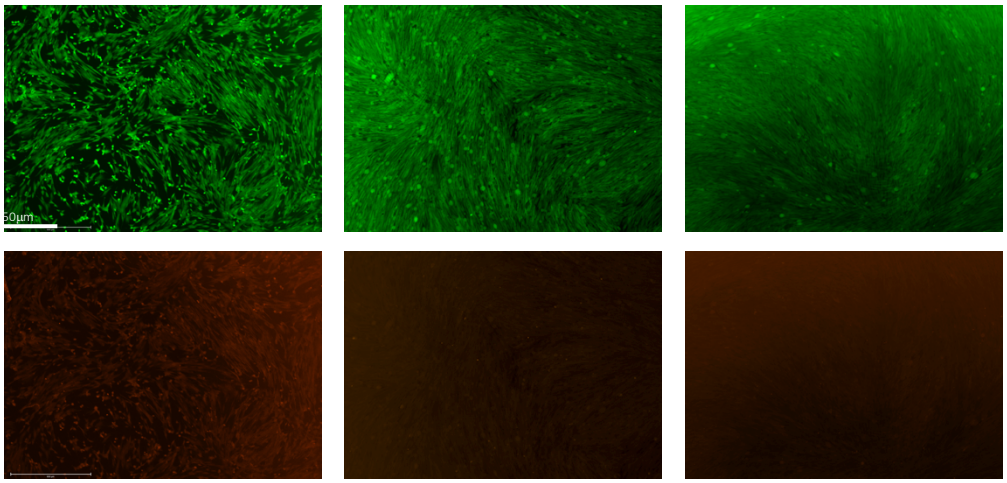		

IIZK

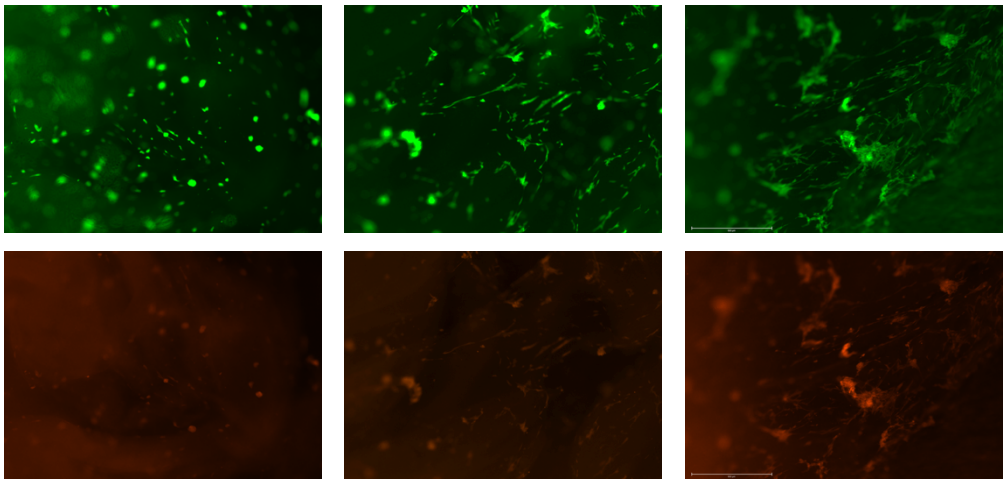

PEP1

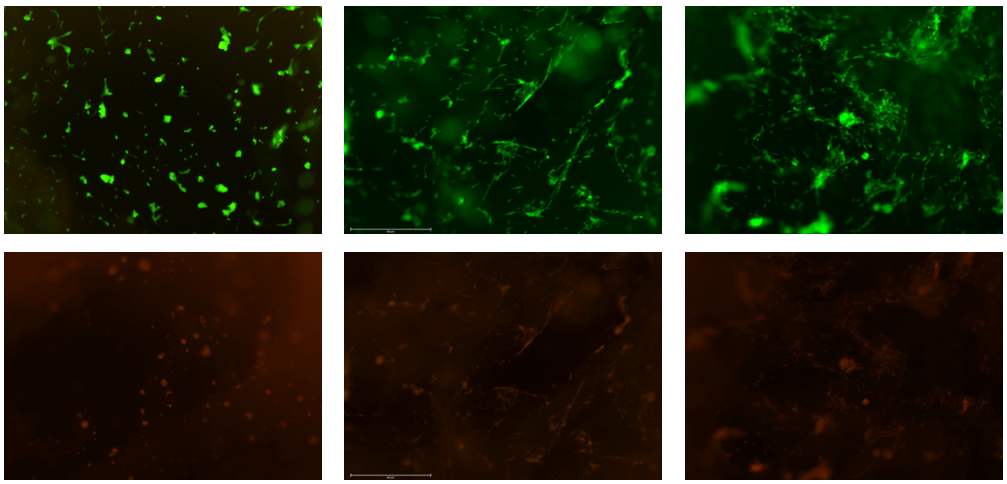

PEP2

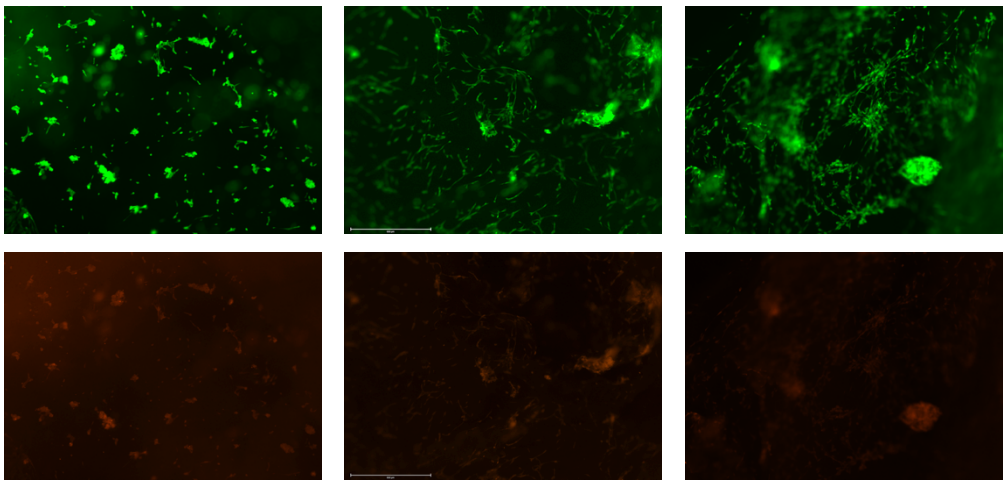

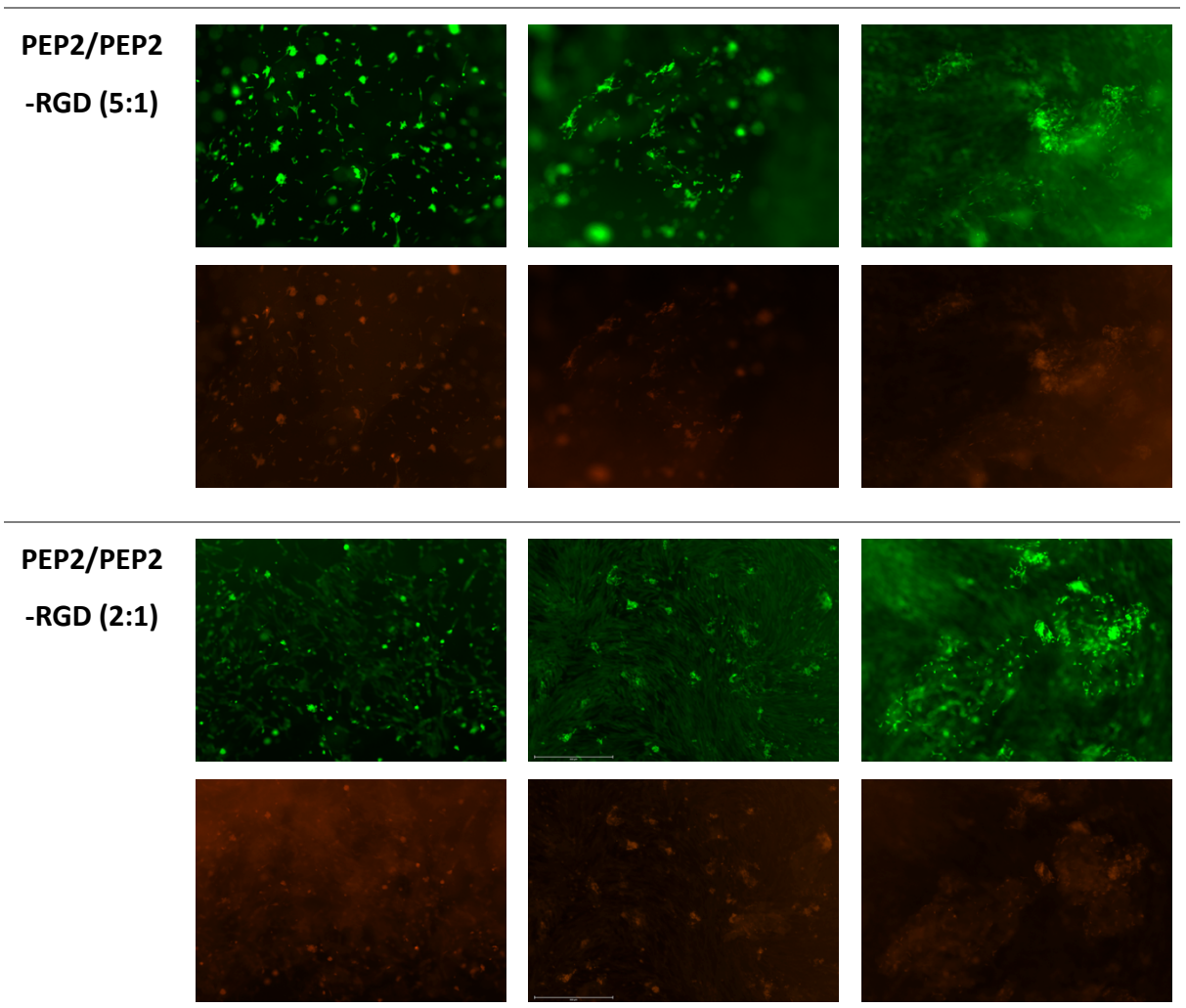

Figure 10. Live/dead assay (GFP & RFP imaging). HDFs in 2D, IIZK, PEP1, PEP2, PEP2/PEP2-RGD (5:1), PEP2/PEP2-RGD (2:1) cultures on day 1, day 2, day 7. Microscopic image captured at 4x magnification.

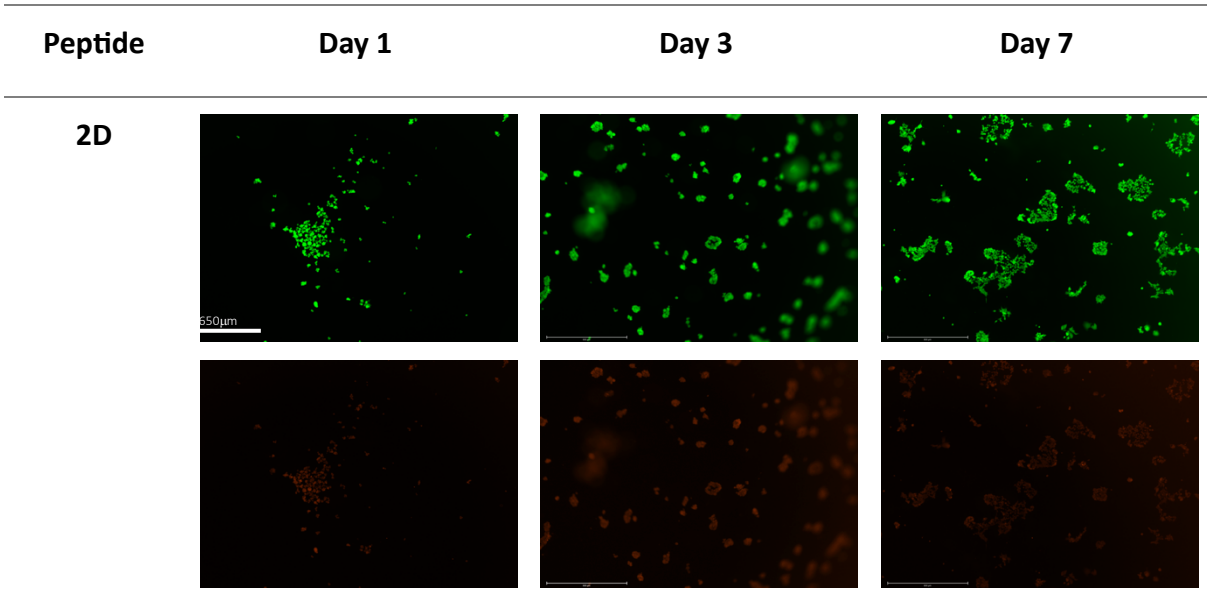

IIZK

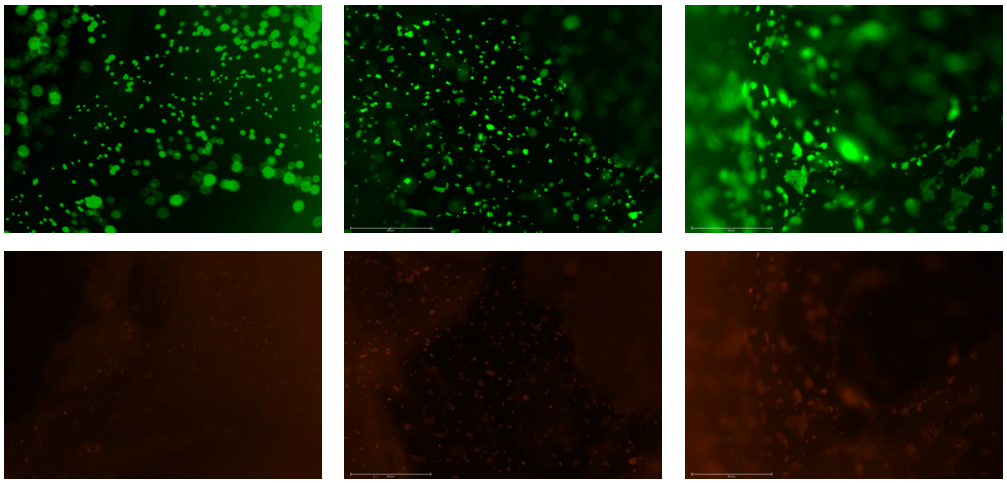

PEP1

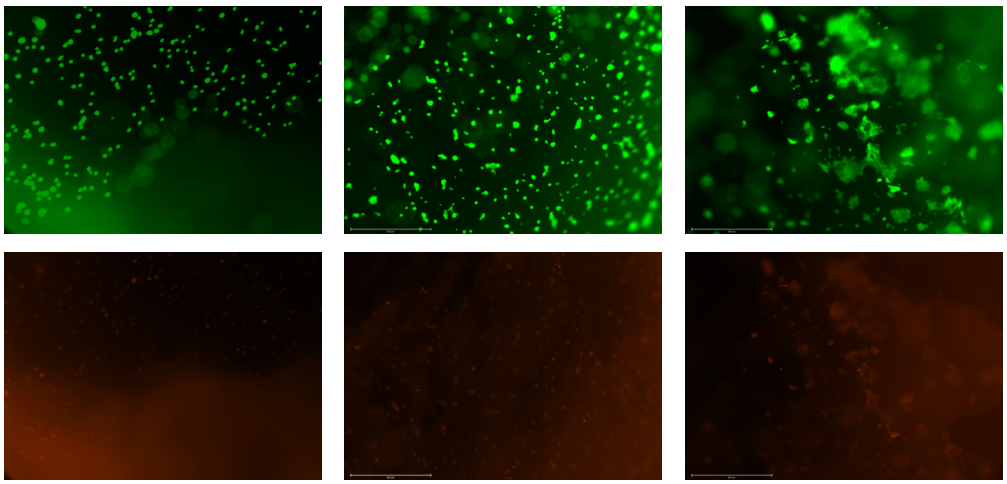

PEP2

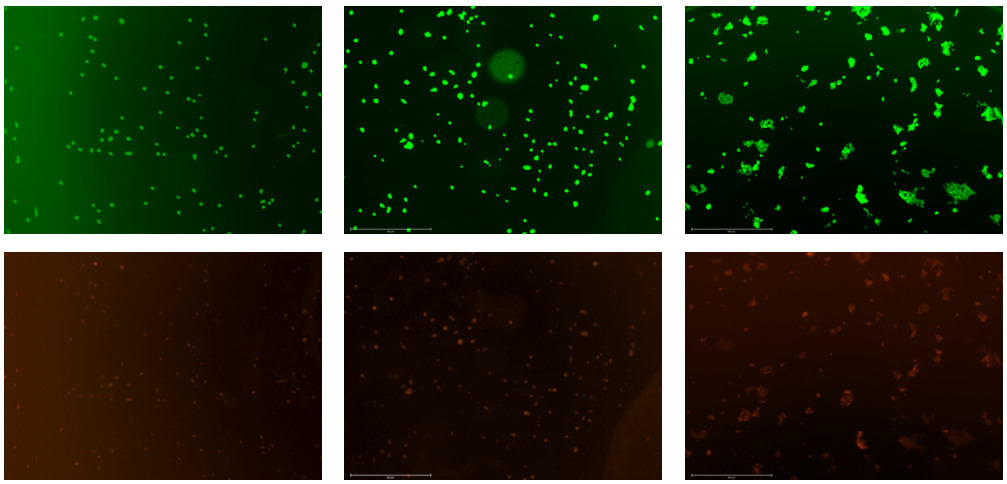

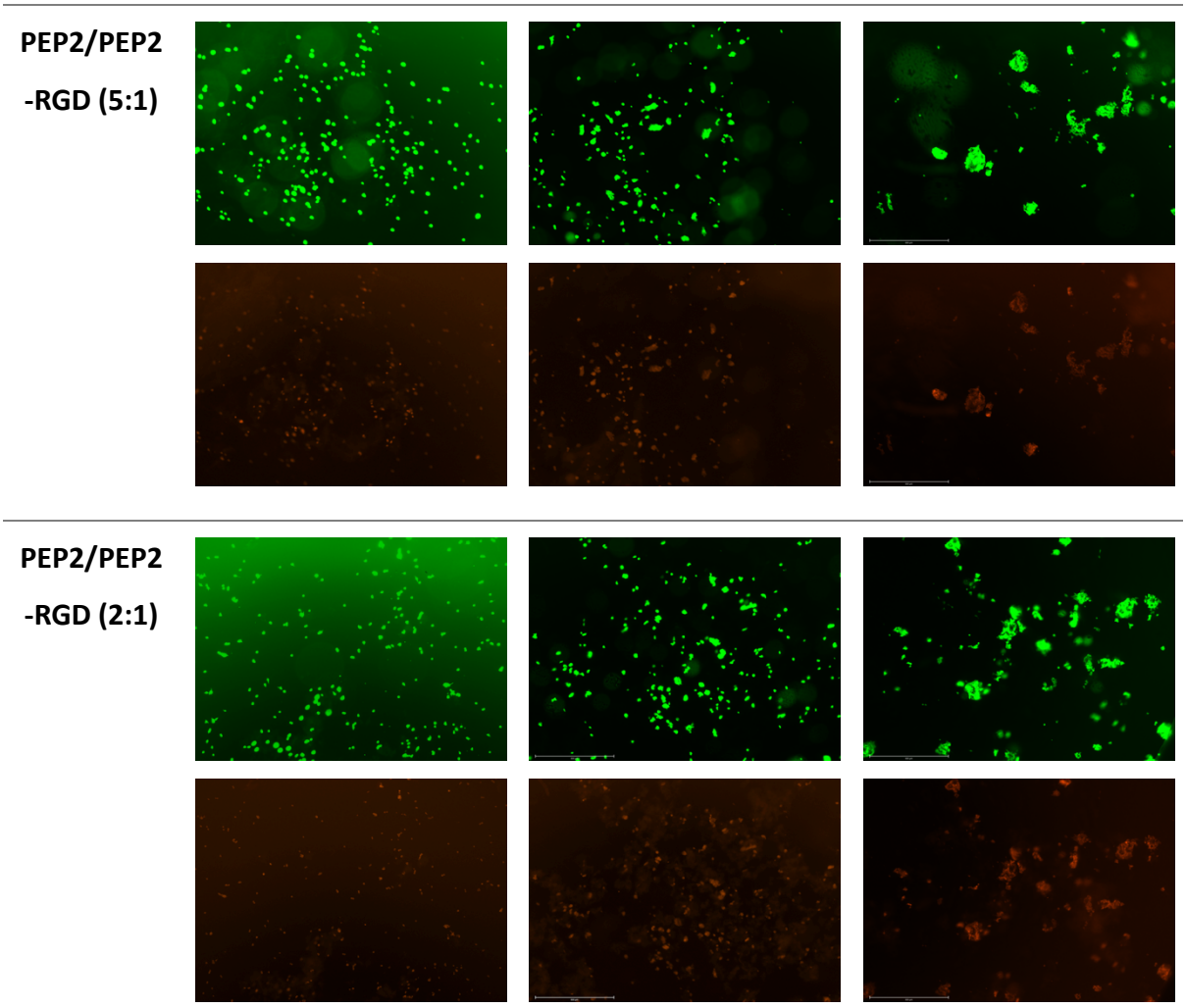

Figure 11. Live/dead assay (GFP & RFP imaging). HEK 293 in 2D, IIZK, PEP1, PEP2, PEP2/PEP2-RGD (5:1), PEP2/PEP2-RGD (2:1) cultures on day 1, day 2, day 7. Microscopic image captured at 4x magnification.

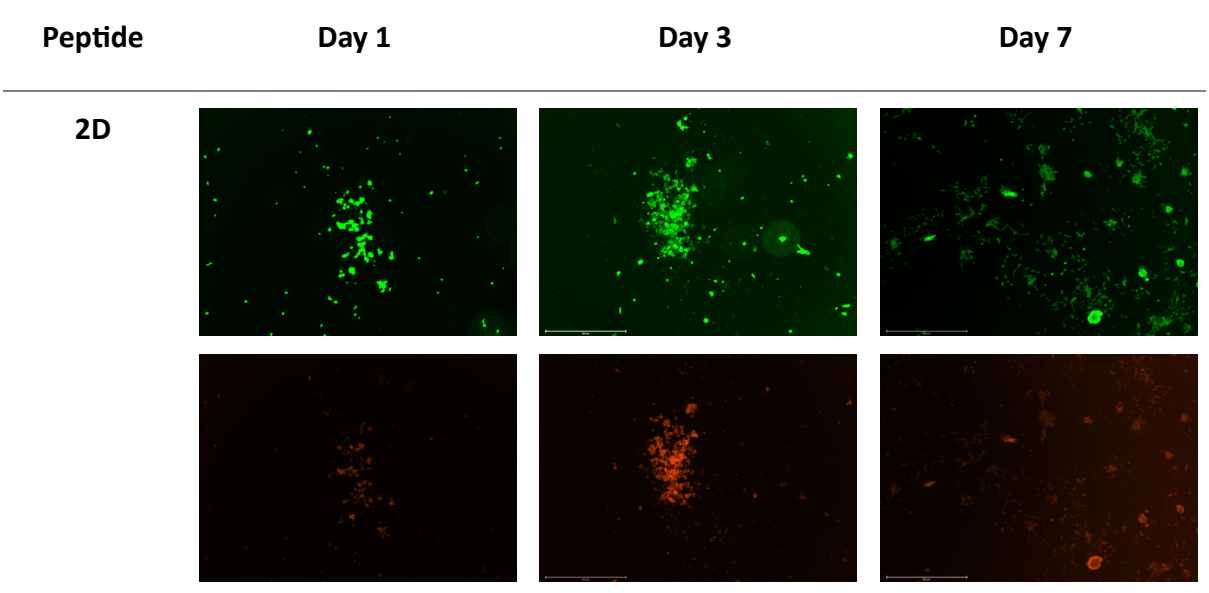

IIZK

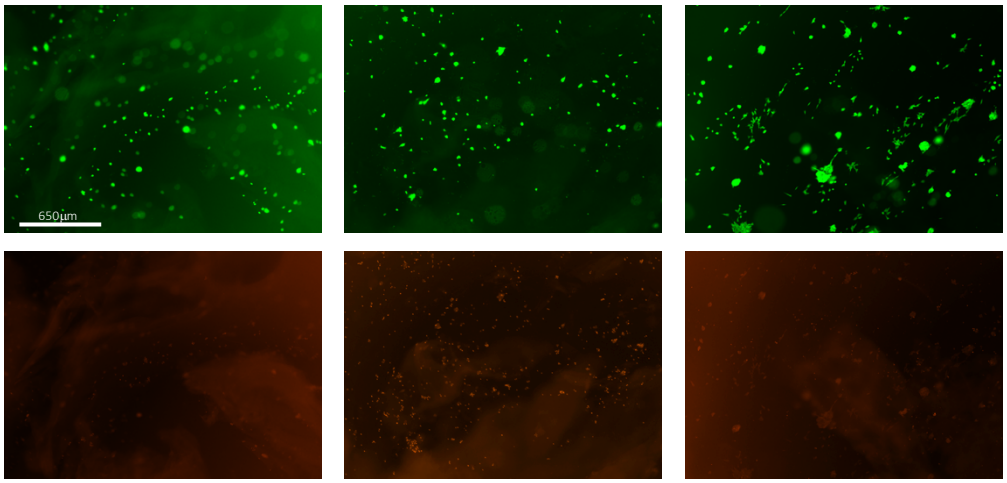

PEP1

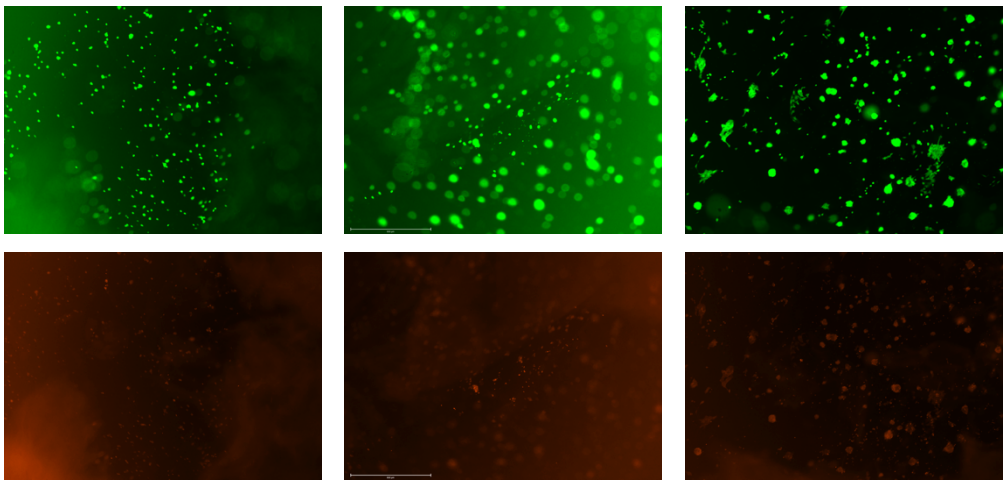

PEP2

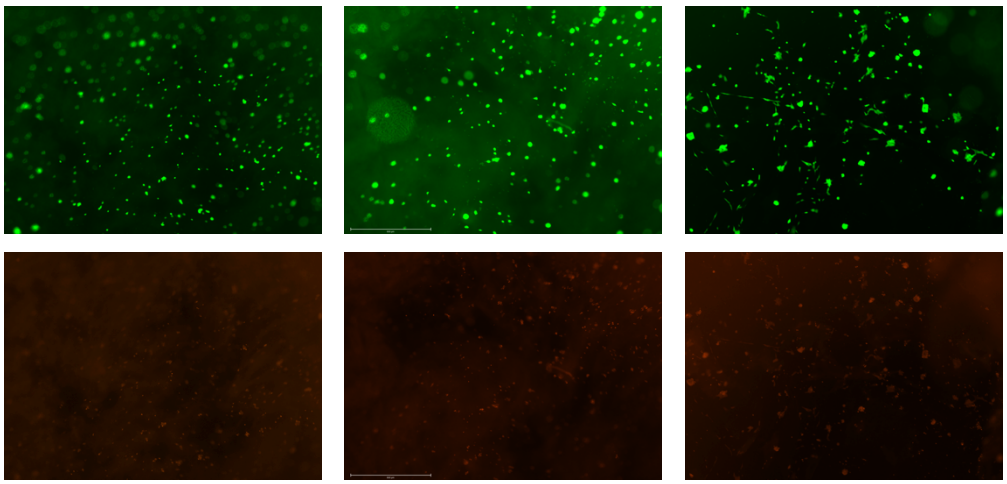

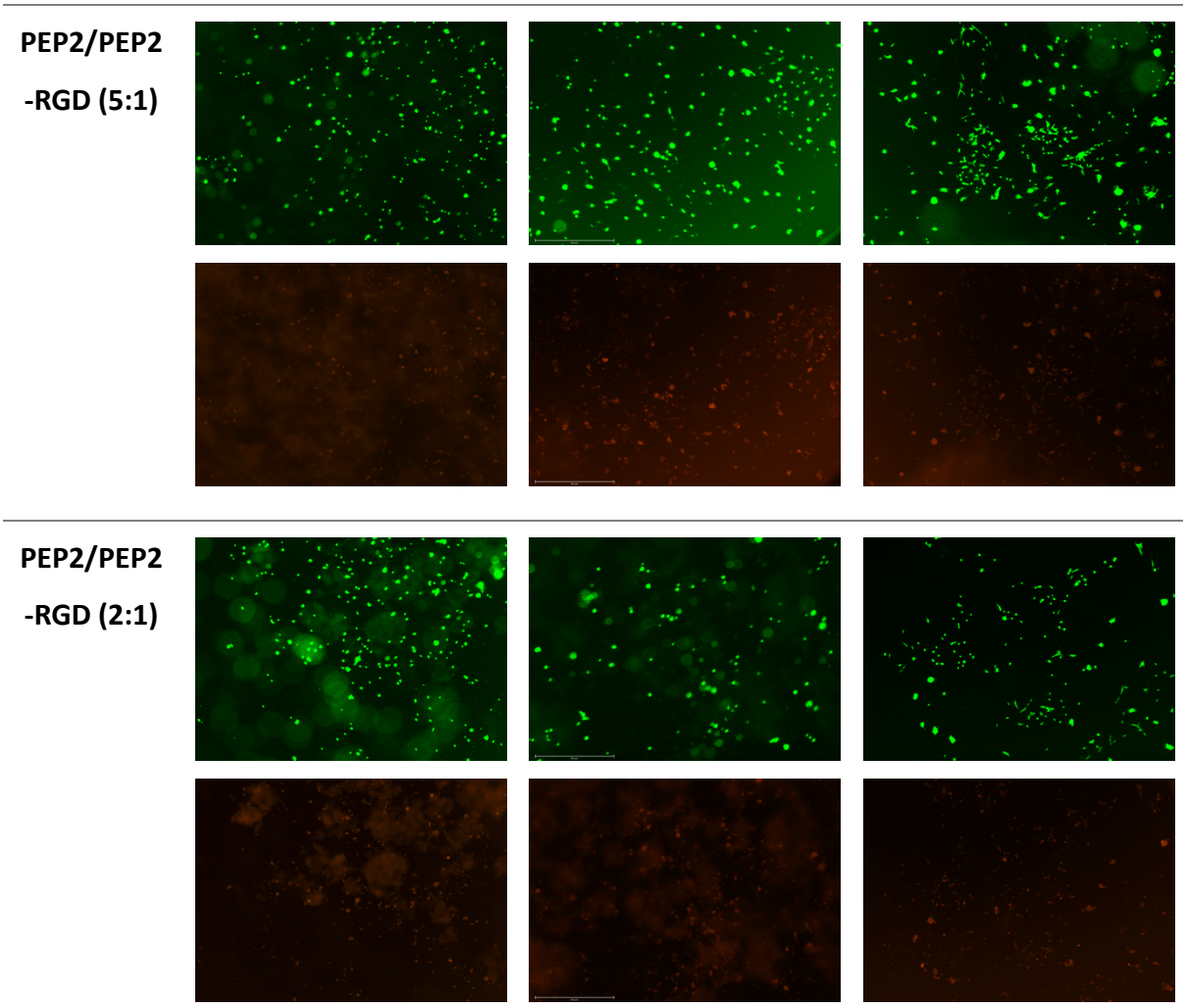

Figure 12. Live/dead assay (GFP & RFP imaging). SH-SY5 in 2D, IIZK, PEP1, PEP2, PEP2/PEP2-RGD (5:1), PEP2/PEP2-RGD (2:1) cultures on day 1, day 2, day 7. Microscopic image captured at 4x magnification.

At an early stage, the cells appear as bright green, due to a highly metabolically active state and an intact cell membrane. This is indicative of a high viability and functionality. A low number of bright red dots is indicative of a few of dead cells. This can be attributed to normal cellular processes. Over time, there is a significant increase in live cells density. The cells cluster and almost cover the whole well area. The increase in cellular activity is noticeable. The number of dead cell didn't increase significantly.

In 3D culture, the observable morphology and behavior evolutions differ from those in 2D culture as the spatial organization goes from planar to a three-dimensional environment. The access to nutrients is lower compared to 2D culture where all the cells are in direct contact with media.

Initially, the cells appear havinng high viability and functionality. Cluster of cells are present which indicates cell-cell communication. A few red dots are visible, mainly in the clusters, indicative of a low number of dead cells. The cells look smaller due to a weaker access of the nutrients inside the gel. They look more spread than in 2D culture.

Over time, there is an increase in live cells density. Most of the green clusters look larger. This suggests a high level of cell viability and functionality within the 3D matrix. Scattered areas of red fluorescence emerge in the cell clusters due to normal cellular processes.

In the other peptides at early stage, the cells appear similar to the control. Overtime, cells seem follow the same evolution with notable increases in population, especially for the HDF and HEK293. SH-SY5 shows a stabilization of the viability between day 3 and day 7. We can conclude that all the peptides showed the capacity to maintain the cell viability over time.

4.2.2. Confirmation of the viability by ATP assay

The cell viability results were confirmed by an ATP assay. Initially, all the cells were seeded at an initial density of 2000 cells per well for each type of cells, the luminescence (RLU) is plotted Figure 15, Figure 14, and Figure 15 for day 1, day 3 and day 7, respectively.

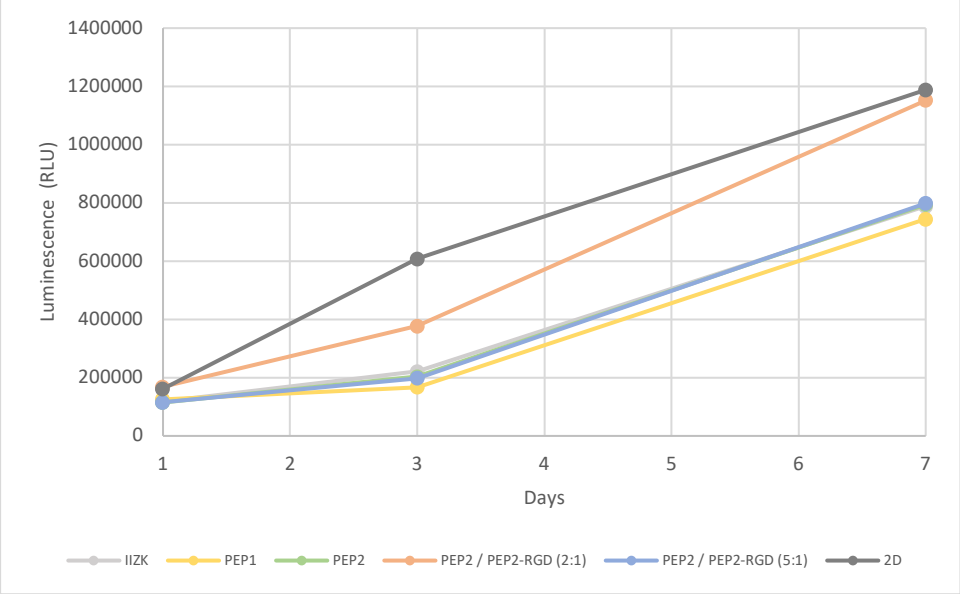

Figure 13. ATP assay. Cells viability evaluation for HDF. Results on day 1, day 3, day 7.

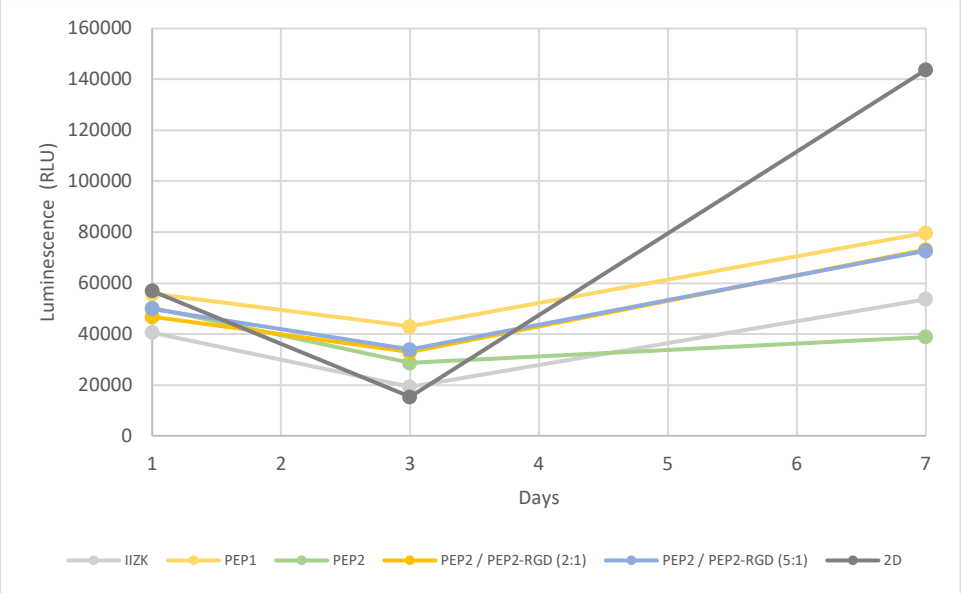

Figure 14. ATP assay. Cells viability evaluation for HEK 293. Results on day 1, day 3, day 7.

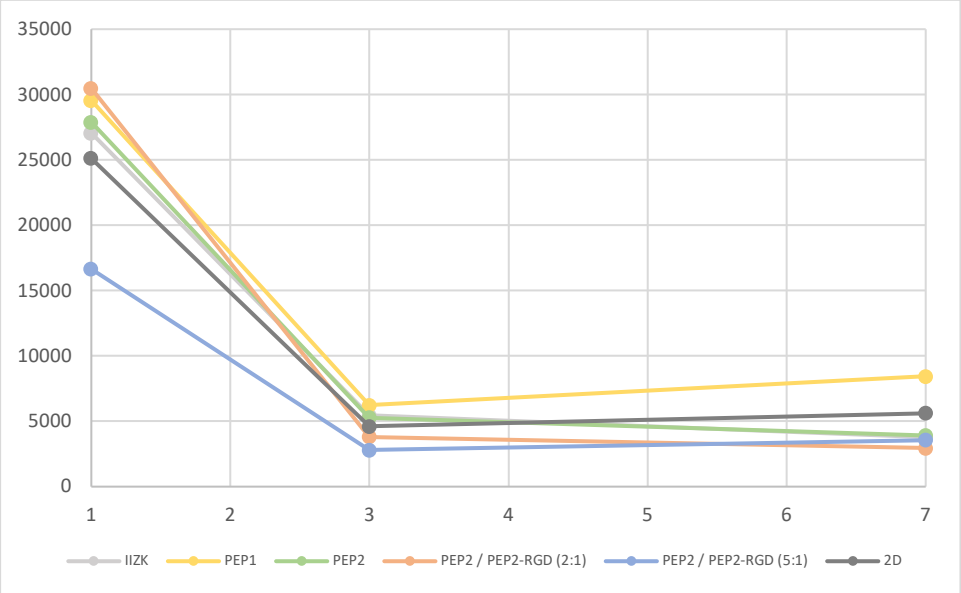

Figure 15. ATP assay. Cells viability evaluation for SH-SY5. Results on day 1, day 3, day 7.

In Figure 13, we notice a continuous increase in luminescence, thus in HDF viability through the days.

Initially, all the peptides showed close values of luminescence (around 130 000 RLU). On day 3, the curves start to differentiate. The 2D culture and PEP2/PEP2-RGD (2:1) showed the highest rates of ATP (luminescence values of 608000 RLU and 377000 RLU respectively). The other peptides IIZK, PEP2/ PEP2-RGD (5:1) and PEP1 reached lower

values (respectively 221000 RLU, 198000 RLU and 167000 RLU). The highest number of viable cells was obtained for the 2D culture. The peptide showing the highest viability was PEP2/PEP2-RGD (2:1), the lowest was PEP1, closely to the other peptides. On day 7, the order remains the same with an increase in cell growth rate for PEP2/PEP2-RGD (2:1) with luminescence values that almost reach the luminescence values for the 2D. The other peptides present similar viabilities, lower than the control.

The HEK 293 cells show a different viability evolution in Figure 14. In the first phase, a similar decrease luminescence shows a diminishing cell viability (from a range of [40 000; 60000]RLU to [19000; 43000] RLU) for all peptides. The 2D culture presents a higher decline, thus we can state that the peptide helps the cell to maintain its viability. In the second phase, the number of cells increases. The 2D culture shows the highest viability recuperation (144000 RLU on day 7). The other peptides presented lower increments in viability ([38000; 80000] RLU).

The evolution of SH-SY5 cells also present a different tendency in Figure 15. Initially, the luminescence values drop drastically. This indicates a notable reduction in viability. From day 3 to day 7, the number of cells increases slightly for all the conditions, except for PEP2/PEP2-RGD (2:1) and PEP2that show a small decline. According to the curves tendencies, the cell division is mainly dictated by the cell. The functionalization RGD seems to enhance the proliferation for certain types of cells. The cells seem to prefer a 2D environment.

In conclusion, all the peptides demonstrated capacity in maintaining the cells viability. The ATP results confirmed the observations obtained from the live/dead assay. The evolution in viability over time does not seem to depend on the amino acids sequence but rather on the cells themselves.

4.2.3. Cytoskeleton analysis

Cytoskeleton staining was performed to further evaluate the biocompatibility of the cells in the peptide hydrogels by analyzing their morphology and interaction of with the material. The results are presented in Figure 16, Figure 17 and Figure 18.

Peptide	Day 1	Day 3	Day 7

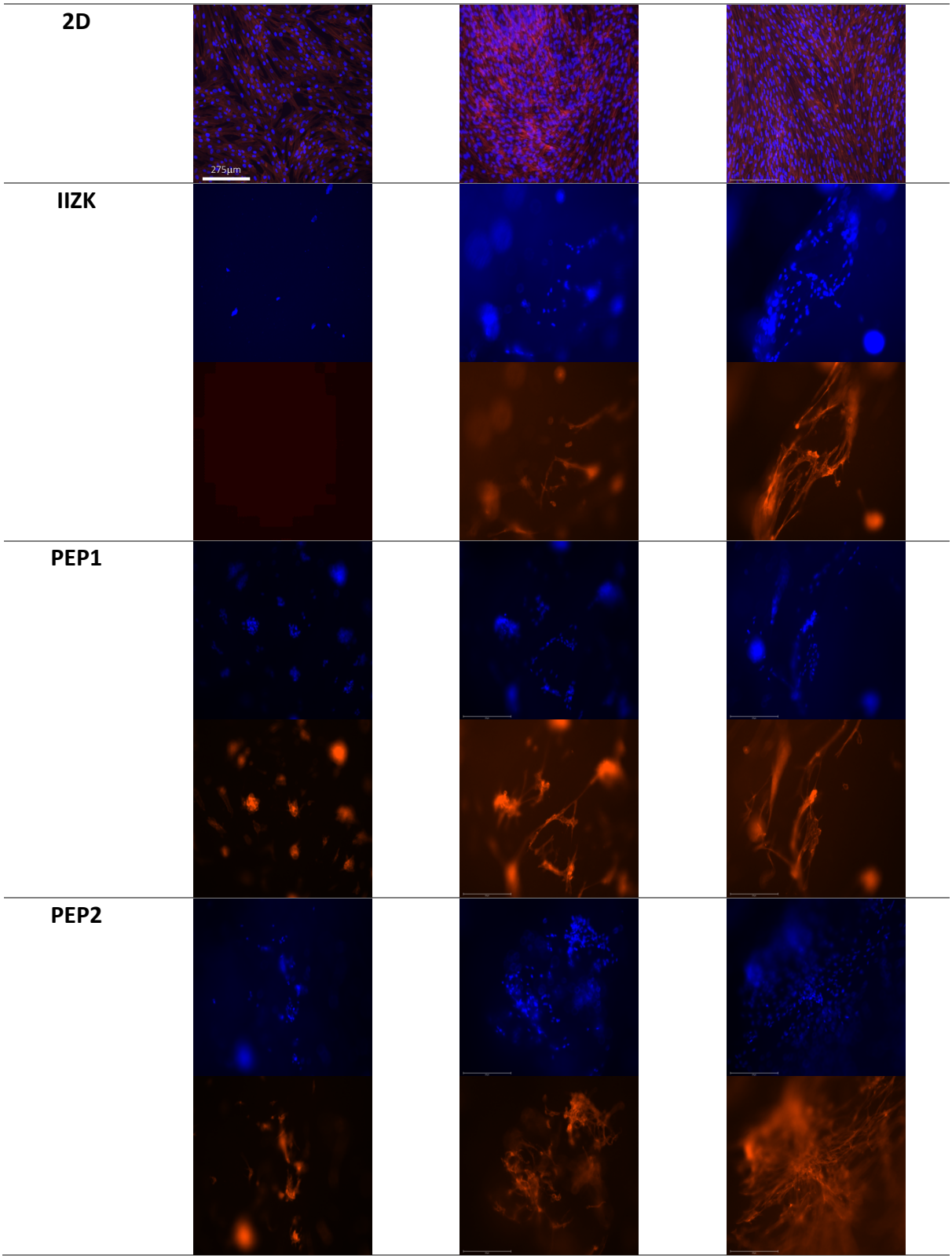
2D
275µm
IIZK
PEP1
PEP2

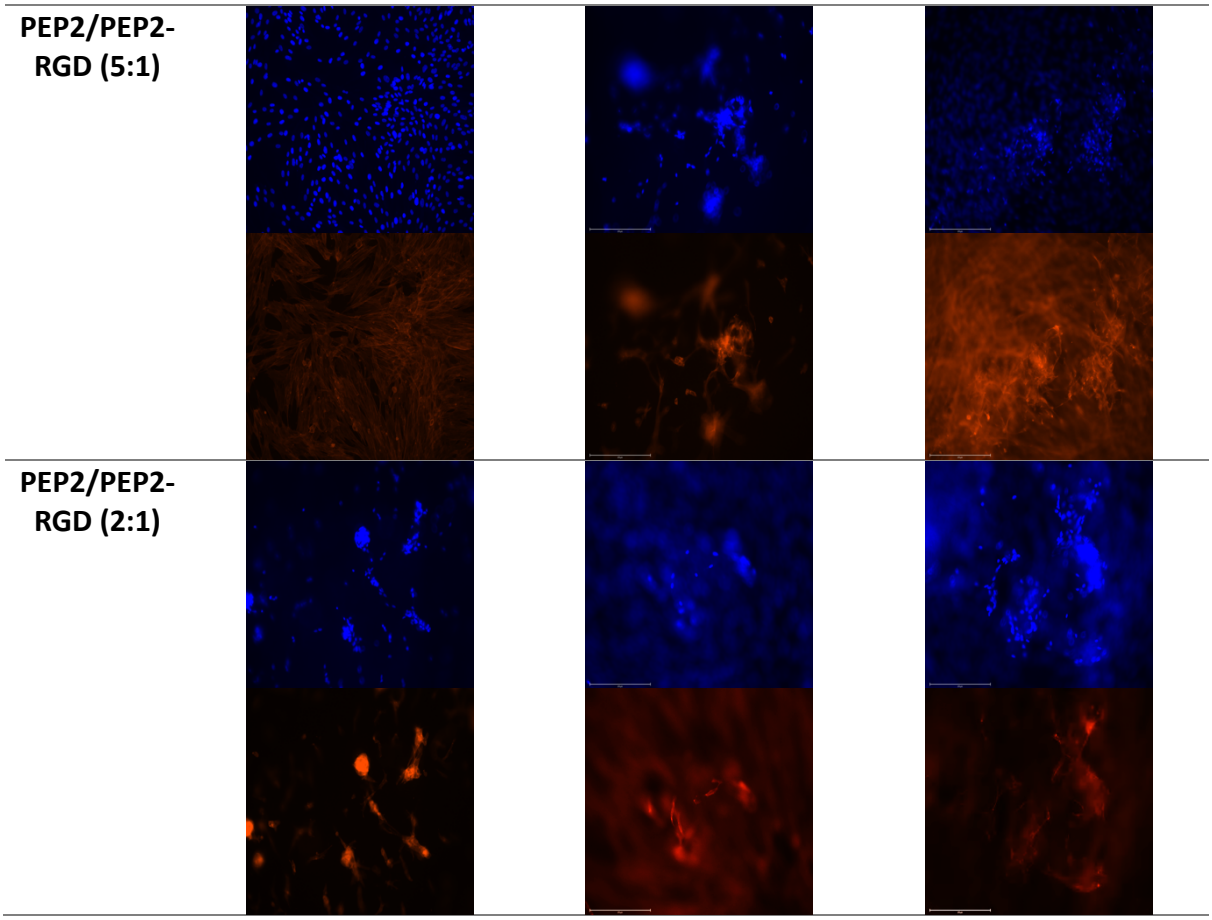

Figure 16. Immunofluorescence staining of the HDFns nucleus (blue) and cytoskeleton protein F-actin (red). Microscopic image captured at 10x magnification

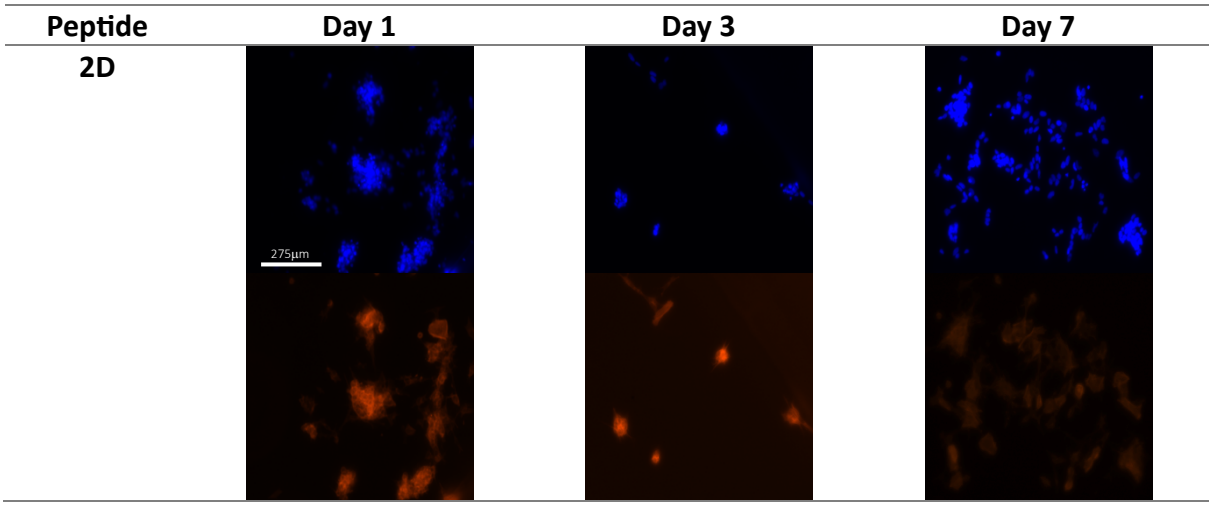

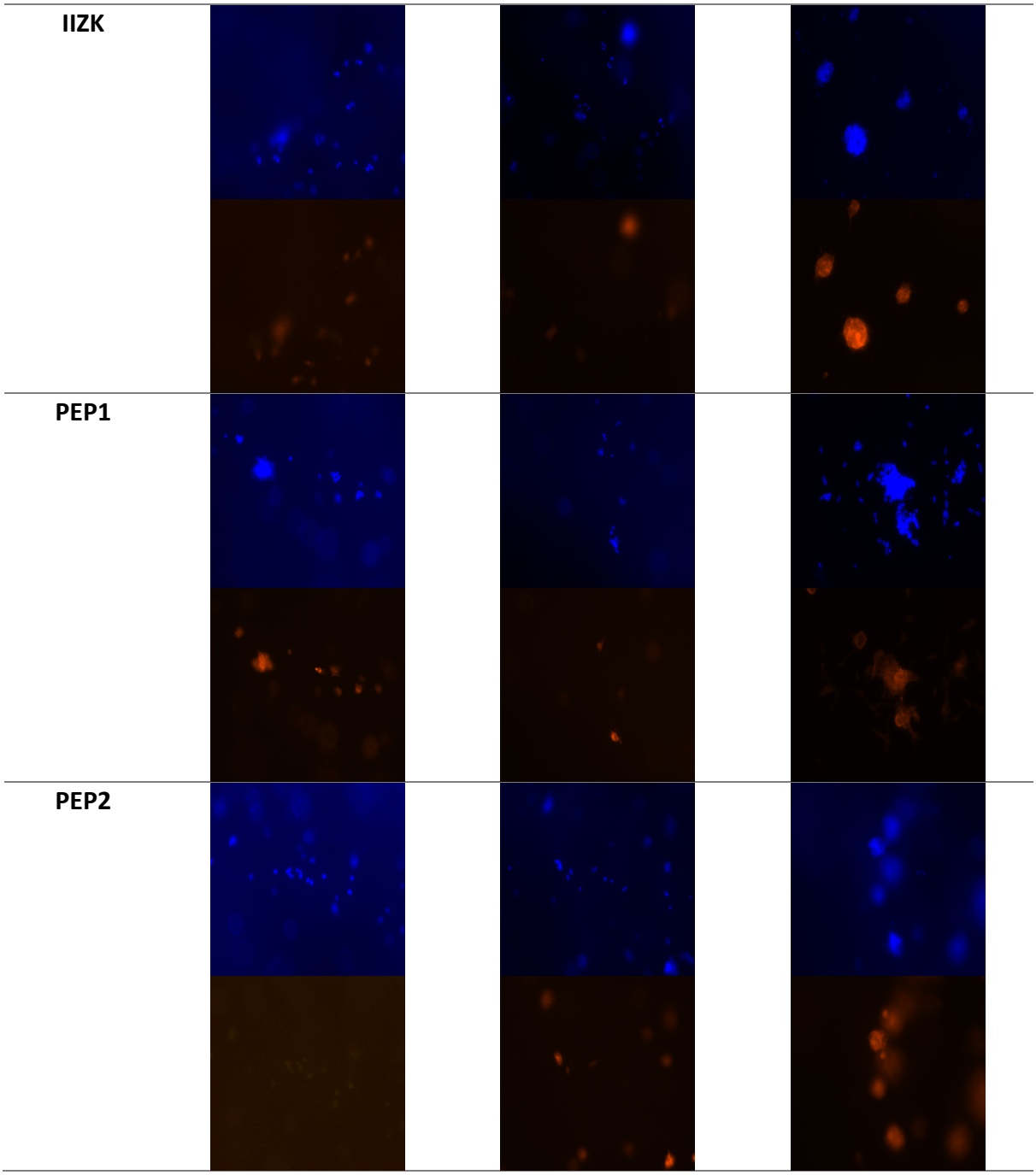
IIZK
PEP1
PEP2

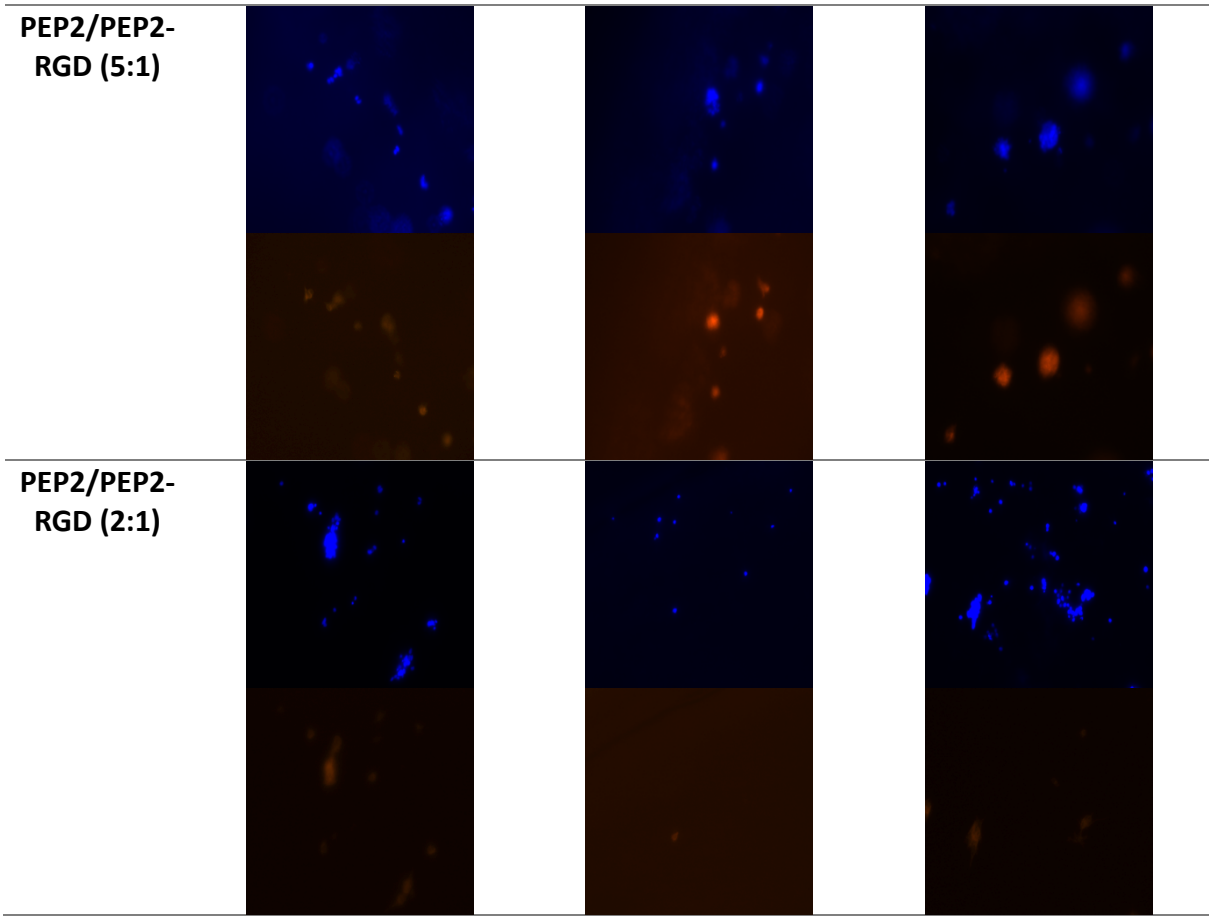

Figure 17. Immunofluorescence staining of the HEK293 nucleus (blue) and cytoskeleton protein F-actin (red). Microscopic image captured at 20x magnification

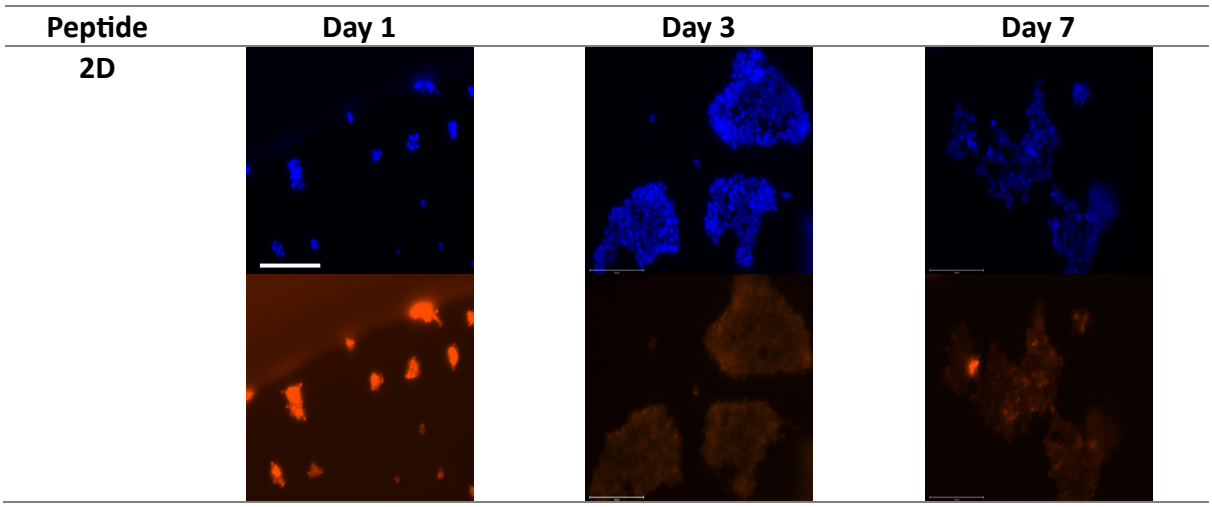

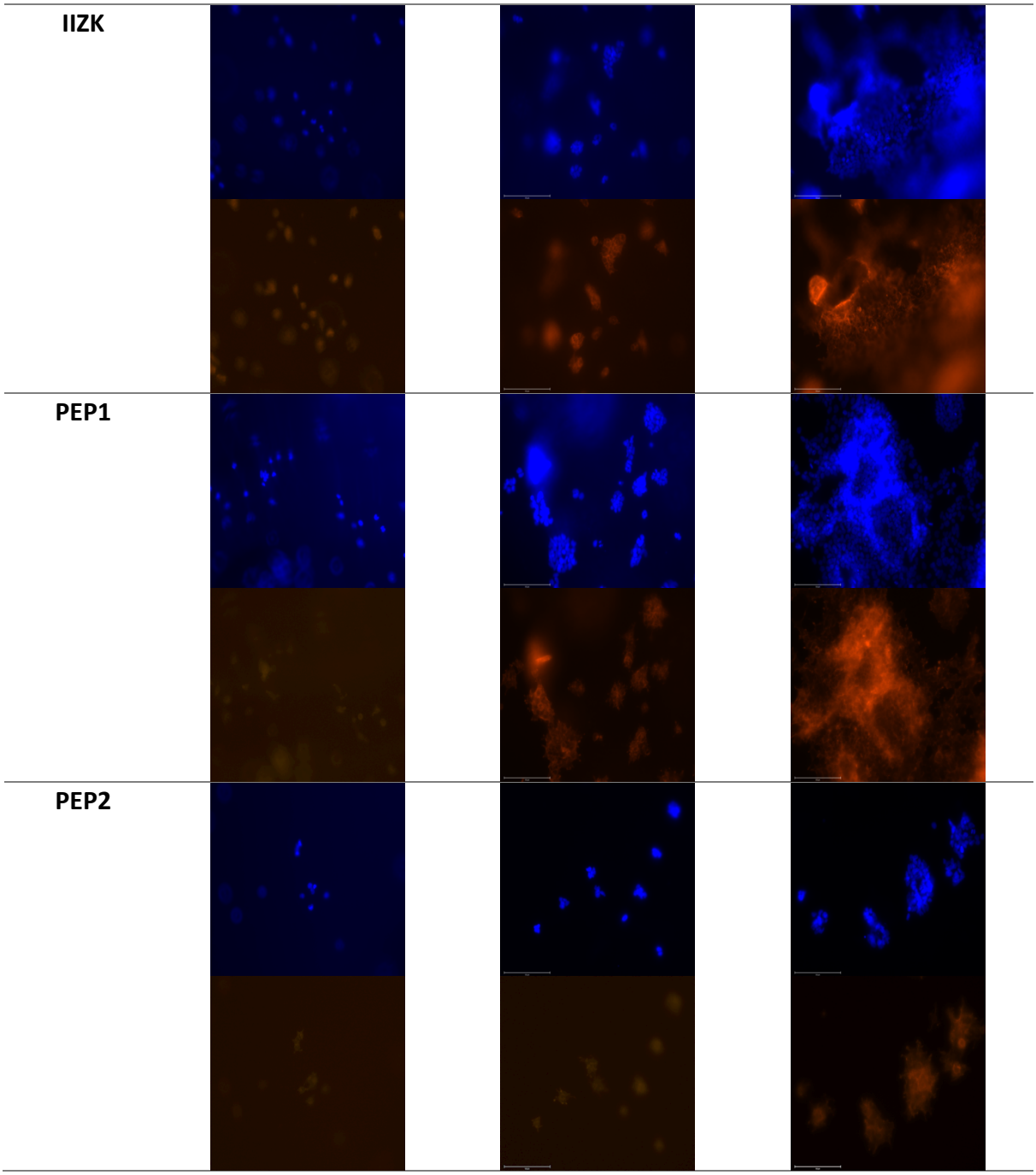
IIZK
PEP1
PEP2

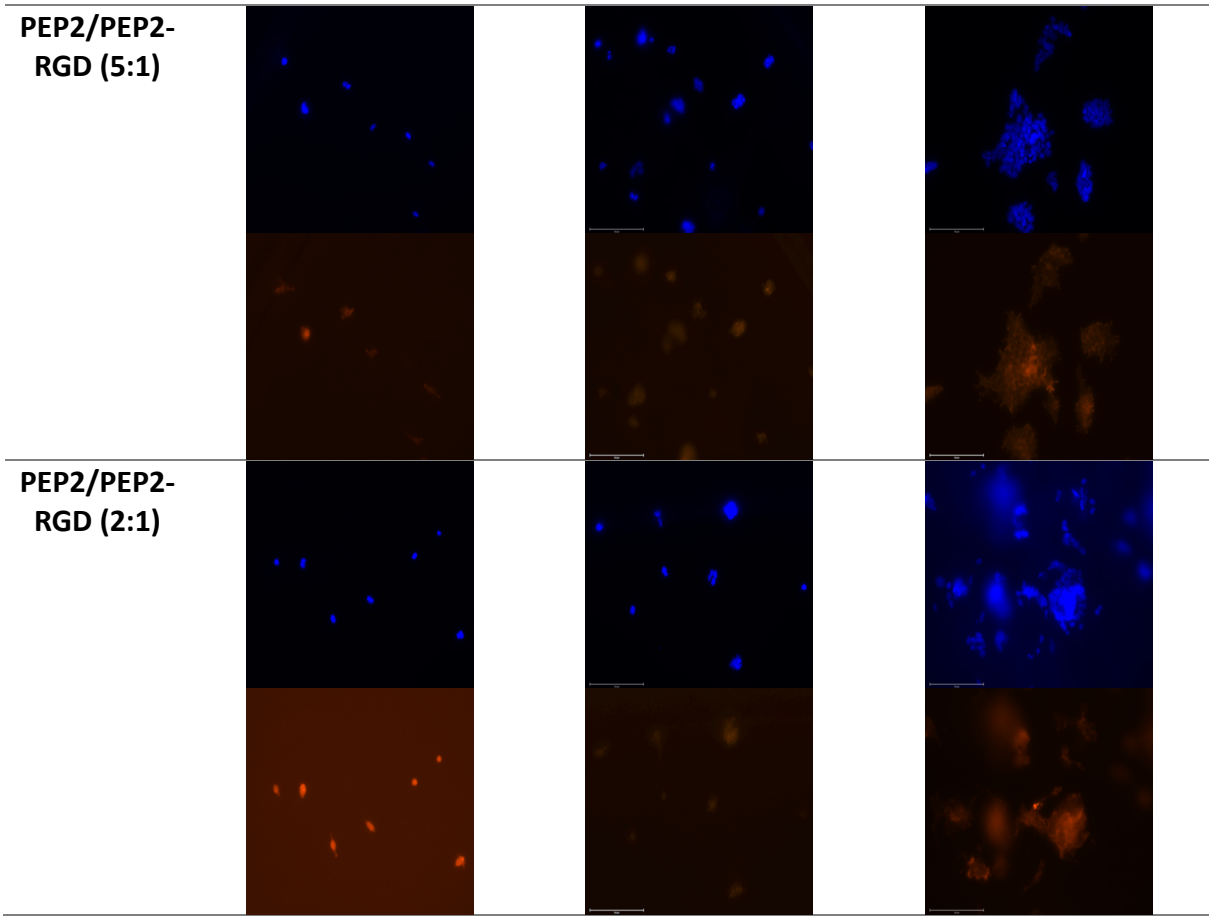

Figure 18. Immunofluorescence staining of the SH-SY5 nucleus (blue) and cytoskeleton protein F-actin (red). Microscopic image captured at 20x magnification.

As illustrated, the morphologies of the cells indicate the presence of F-actin filaments, which provides mechanical support, in all the peptides. This indicates cell-matrix interaction. Based on these results, we can conclude that all the peptides are favorable environments for the cells and confirms the non-cytotoxicity of the materials.

4.3. Influence of the peptide inks on the 3D printing

4.3.1. Printability assessment: initial screening and printing parameters

According to the tests presented in Table 4, the optimal parameters for 3D printing of peptide constructs were defined as: 10 $mg.mL^{-1}$ for the peptide concentration, 5X PBS for the gelation inducer. Flows were determined for each peptide in Section 4.3.1.

4.3.2. Comparison of the ultrashort peptides influence on the printing process

The peptides gelation times in the nozzle are presented in Table 6. Gelation time evaluation in the printing system for decreasing flows or concentrations. The peptide flows

were decreased gradually to reach the lowest concentration possible in the 3D structures. The results are presented in bold. IIZK presents good results at 55 µL/min. PEP1 and PEP2showed gelation times close to IIZK's at 45 µL/min. Functionalized peptides mixtures showed low gelation times or no gelation at lower flows.

Table 6. Gelation time evaluation in the printing system for decreasing flows or concentrations. (Optimal: green ; Acceptable: yellow ; Not suitable). For the stiffness, optimal means a regular, thin and stiff thread. For the clogging, it means that the ink flows continuously. For the resolution, it means that the thread is defined and regular.

Peptide	Concentration ($mg.mL^{-1}$)	PBS	Pump flows (µL/min)			Gelation time (h:min:s)	Observations		
			Pump 1 (peptide)	Pump 2 (PBS)	Pump 3 (1X PBS)		Stiffness	Clogging	Resolution
IIZK	13	5X	55	15	15	00:00:30			
	10					**00:00:45**			
	8					00:01:15			
PEP1	10	5X	55	15	15	00:00:45			
	10		50	15	15	00:00:55			
	10		**45**	**15**	**15**	**00:01:00**			
PEP2	10	5X	50	15	15	00:00:55			
	10		**45**	**15**	**15**	**00:01:00**			
PEP2/ PEP2-RGD (5:1)	10	5X	50	15	15	00:25:00			
	10		45	15	15	00:30:00			
	10		40	15	15	00:35:00			
	10		35	15	15	00:35:00			
PEP2/ PEP2-RGD (2:1)	10	5X	40	15	15	00:25:00			
	10		35	15	15	00:30:00			

4.3.3. Comparison of the peptides influence on the scaffold properties.

Two types of constructs were printed: a square spiral and a cylinder. The objective is to evaluate the continuity, the regularity, the resolution and the shape fidelity of each peptide during the printing. The flow rates were determined previously. The values for IIZK, PEP1 and PEP2 are presented in Table 6. Gelation time evaluation in the printing system for decreasing flows or concentrations. The peptides that didn't meet the gelation time requirements were tested at flow rates of 50/15/15 µL/min. The results are presented in Figure 19.

Peptide	**Spiral**	**Cylinder**

IIZK	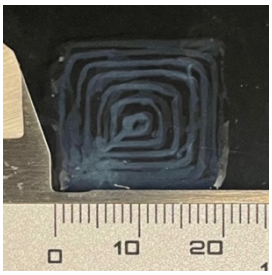	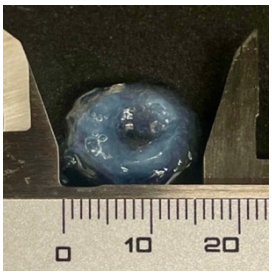
PEP1	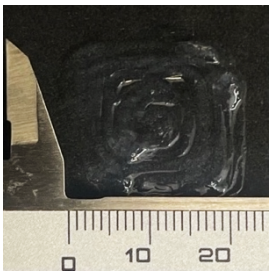	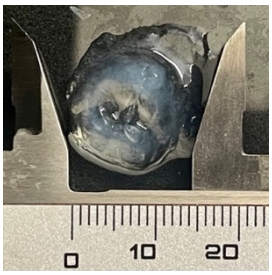
PEP2	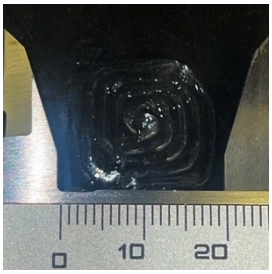	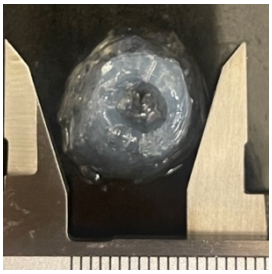
PEP2/ PEP2-RGD (5:1)		NOT PRINTABLE
PEP2/ PEP2-RGD (2:1)	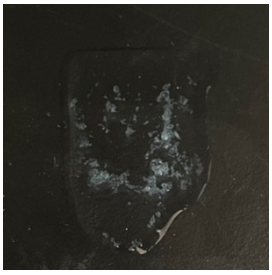	NOT PRINTABLE

Figure 19. 3D printing for resolution, continuity, regularity, and shape fidelity evaluation. Printings of 2x2 cm square spiral and ⌀2cm cylinder (20 layers) for IIZK (control), PEP1, PEP2, PEP2/PEP2-RGD (5:1) and PEP2/ PEP2-RGD (2:1).

The square shape and the cylinder showed a high resolution with continuous, regular and defined lines in IIZK, PEP1 and PEP2. The measurements show a high fidelity to the digital model.

IIZK, PEP1 and PEP2printed smoothly with no clumps or clogging observed, resulting in a continuous thread. The layers were deposited without any dragging of the previous layers. PEP1 and PEP2seem to be clearer than IIZK. PEP2showed the most definition and depth of them all.

With functionalized peptides, there was no resolution. Numerous clumps were observed, causing significant discontinuities or no lines. Only clumps were deposited. No layers can be seen. Flow rates of 45/15/15 µL/min and 40/15/15 µL/min were tested, unsuccessfully. Thus, the cylinders could not be printed.

4.4. Cells behaviour in the 3D bioprinted constructs

The peptides that proved to be suitable for 3D printing were used to extrude cellularized scaffold. Fibroblasts were chosen for their adaptability to variability in conditions. Live/dead assay was performed on the 3D bioprinted constructs to evaluate the viability of the cells in after 3D printing. The results are presented in Figure 20.

Peptide	Day 1	Day 3	Day 7
IIZK	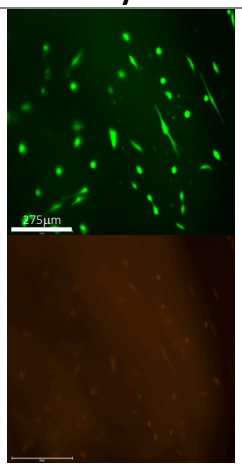		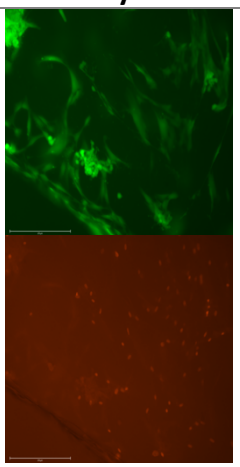

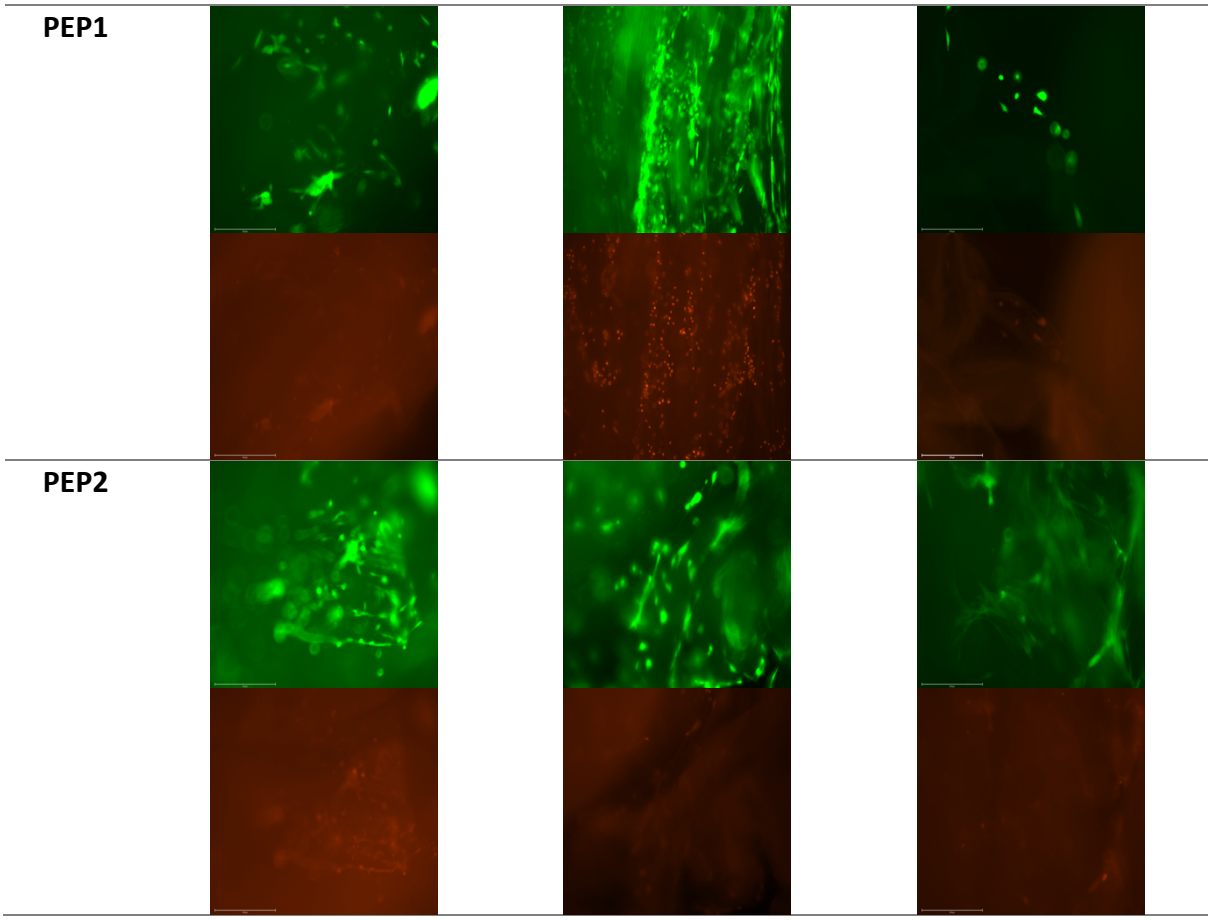

Figure 20. Live/dead assay (GFP & RFP imaging). HDFin IIZK, PEP1, PEP2constructs on day 1, day 2, day 7. Microscopic image captured at 10x magnification.

First, we notice high discrepancies in cell density between constructs with no cells in the IIZK construct on day 3 and a very high cell density in the PEP1 construct of day 3. This is caused by the printing setup which is not fully optimized and delivers variable amounts of cells over time despite due to an uneven distribution of cells in pump 3.

Nonetheless, for the constructs that present cells, they appear as bright green, and a few red dots, indicating of a high viability and functionality. In the early stages the cells look spread. The green background suggests that cells are presents in the bottom layers of the constructs. Over time, the cells seem to develop normally as they do in non-printed 3D culture (Section 4.2.1). We can conclude that the printing process itself doesn't affect the cell viability, but the setup needs to be optimized to obtain a regular distribution of the cells through the entire 3D matrix.

5. Conclusion

The potential of four new self-assembling peptides (PEP1, PEP2, PEP2-RGD) as a scaffold for 3D organoids was established. The mechanical properties of each self-assembling peptide were characterized.

First, a gelation test was performed to assess their ability to form a stable hydrogel under controlled conditions. Following the gelation, rheological measurements were conducted to determine the viscoelastic behavior of each hydrogel, including their elasticity and stiffness. PEP1 and PEP2showed similar behaviors to the control, IIZK. Moreover, the SAPs' ability to maintain cell viability was successfully assessed by evaluating the evolution of three types of cells (HDFs, HEK293, SH-SY5) through live/dead staining, ATP assay and cytoskeleton imaging. All the tested peptides demonstrated biocompatibility and absence of cytotoxicity. In addition, the SAPs were tested as bioinks in a 3D printing system. The resolution and smoothness of the process were evaluated, and favorable results were obtained for PEP1 and PEP2. Lastly, the selected peptides were used to as a bioink to print cellularized constructs to prove their potential as new materials for 3D organoids development, successfully.

These newly characterized peptides can now be used by the Hauser group to continue the research around organoids using new in-house developed biomaterials as scaffolds.

6. References

1. Jensen, C. and Y. Teng, *Is It Time to Start Transitioning From 2D to 3D Cell Culture?* Front Mol Biosci, 2020. **7**: p. 33.
2. Alzanbaki, H., M. Moretti, and C.A.E. Hauser, *Engineered Microgels-Their Manufacturing and Biomedical Applications.* Micromachines (Basel), 2021. **12**(1).
3. Susapto, H.H., et al., *Ultrashort Peptide Bioinks Support Automated Printing of Large-Scale Constructs Assuring Long-Term Survival of Printed Tissue Constructs.* Nano Lett, 2021. **21**(7): p. 2719-2729.
4. Kim, S., et al., *Tissue extracellular matrix hydrogels as alternatives to Matrigel for culturing gastrointestinal organoids.* Nat Commun, 2022. **13**(1): p. 1692.
5. Souza, N.d., *Organoids.* Nature Methods, 2018. **15**(1): p. 23-23.
6. Hofer, M. and M.P. Lutolf, *Engineering organoids.* Nat Rev Mater, 2021. **6**(5): p. 402-420.
7. Matsui, T. and T. Shinozawa, *Human Organoids for Predictive Toxicology Research and Drug Development.* Front Genet, 2021. **12**: p. 767621.
8. Susaki, E.A. and M. Takasato, *Perspective: Extending the Utility of Three-Dimensional Organoids by Tissue Clearing Technologies.* Front Cell Dev Biol, 2021. **9**: p. 679226.
9. Kim, J., B.K. Koo, and J.A. Knoblich, *Human organoids: model systems for human biology and medicine.* Nat Rev Mol Cell Biol, 2020. **21**(10): p. 571-584.
10. Tang, X.Y., et al., *Human organoids in basic research and clinical applications.* Signal Transduct Target Ther, 2022. **7**(1): p. 168.
11. Artegiani, B. and H. Clevers, *Use and application of 3D-organoid technology.* Hum Mol Genet, 2018. **27**(R2): p. R99-R107.
12. Rossi, G., A. Manfrin, and M.P. Lutolf, *Progress and potential in organoid research.* Nat Rev Genet, 2018. **19**(11): p. 671-687.
13. Foley, K.E., *Organoids: a better in vitro model.* Nat Methods, 2017. **14**(6): p. 559-562.
14. Kratochvil, M.J., et al., *Engineered materials for organoid systems.* Nat Rev Mater, 2019. **4**(9): p. 606-622.
15. Poudel, H., et al., *Synthetic Matrices for Intestinal Organoid Culture: Implications for Better Performance.* ACS Omega, 2022. **7**(1): p. 38-47.
16. Cheung, H.-Y., et al., *A critical review on polymer-based bio-engineered materials for scaffold development.* Composites Part B: Engineering, 2007. **38**(3): p. 291-300.
17. de León, E.H.-P., et al., *Intelligent and smart biomaterials for sustainable 3D printing applications.* Current Opinion in Biomedical Engineering, 2023. **26**.
18. Chan, K.H., et al., *Systematic Moiety Variations of Ultrashort Peptides Produce Profound Effects on Self-Assembly, Nanostructure Formation, Hydrogelation, and Phase Transition.* Sci Rep, 2017. **7**(1): p. 12897.

19. Stojkov, G., et al., *Relationship between Structure and Rheology of Hydrogels for Various Applications.* Gels, 2021. **7**(4).

20. Loo, Y., et al., *A Chemically Well-Defined, Self-Assembling 3D Substrate for Long-Term Culture of Human Pluripotent Stem Cells.* ACS Appl Bio Mater, 2019. **2**(4): p. 1406-1412.

21. Perez-Pedroza, R., et al., *Fabrication of lumen-forming colorectal cancer organoids using a newly designed laminin-derived bioink.* Int J Bioprint, 2023. **9**(1): p. 633.

22. Ramirez-Calderon, G., H.H. Susapto, and C.A.E. Hauser, *Delivery of Endothelial Cell-Laden Microgel Elicits Angiogenesis in Self-Assembling Ultrashort Peptide Hydrogels In Vitro.* ACS Appl Mater Interfaces, 2021. **13**(25): p. 29281-29292.

23. Alshehri, S., H.H. Susapto, and C.A.E. Hauser, *Scaffolds from Self-Assembling Tetrapeptides Support 3D Spreading, Osteogenic Differentiation, and Angiogenesis of Mesenchymal Stem Cells.* Biomacromolecules, 2021. **22**(5): p. 2094-2106.

24. Seow, W.Y. and C.A.E. Hauser, *Short to ultrashort peptide hydrogels for biomedical uses.* Materials Today, 2014. **17**(8): p. 381-388.

25. Velasco, V., S.A. Shariati, and R. Esfandyarpour, *Microtechnology-based methods for organoid models.* Microsyst Nanoeng, 2020. **6**: p. 76.

26. Van der Vaart, J. and H. Clevers, *Airway organoids as models of human disease.* J Intern Med, 2021. **289**(5): p. 604-613.

27. Zhao, Z., et al., *Organoids.* Nature Reviews Methods Primers, 2022. **2**(1).

28. Sher, D., *Bioprinting*, in *Breaching new dimensions for biomedical applications*, T. Boissonneault, Editor. 2023, 3dpbm.

29. Sorrell, J.M. and A.I. Caplan, *Fibroblasts-a diverse population at the center of it all.* Int Rev Cell Mol Biol, 2009. **276**: p. 161-214.

30. Hu, J., et al., *Human Embryonic Kidney 293 Cells: A Vehicle for Biopharmaceutical Manufacturing, Structural Biology, and Electrophysiology.* Cells Tissues Organs, 2018. **205**(1): p. 1-8.

31. Sundar, S.J., et al., *Three-dimensional organoid culture unveils resistance to clinical therapies in adult and pediatric glioblastoma.* Transl Oncol, 2022. **15**(1): p. 101251.

32. Alexander, B.M. and T.F. Cloughesy, *Adult Glioblastoma.* J Clin Oncol, 2017. **35**(21): p. 2402-2409.

33. Wirsching, H.-G. and M. Weller, *Glioblastoma*, in *Malignant Brain Tumors : State-of-the-Art Treatment*, J. Moliterno Gunel, J.M. Piepmeier, and J.M. Baehring, Editors. 2017, Springer International Publishing: Cham. p. 265-288.

34. Xicoy, H., B. Wieringa, and G.J. Martens, *The SH-SY5Y cell line in Parkinson's disease research: a systematic review.* Mol Neurodegener, 2017. **12**(1): p. 10.

Appendix

Appendix 1. Minimum gelation concentration. Inverted vial test results

IIZK							
From previous data: < 3 min							
Time (min)	Sample	Concentration (mg.mL^{-1})	State				
			Liquid	Liquid / viscous	Viscous	Viscous / solid	Solid
1	Control	2.00					X
2	Control	2.00					X
3	Control	2.00					X
Minimum gelation concentration: 2 mg.mL^{-1}							

PEP1							
From previous data: < 5 min							
Time (min)	Sample	Concentration (mg.mL^{-1})	State				
			Liquid	Liquid / viscous	Viscous	Viscous / solid	Solid
1	1	1.00	X				
	2	2.00			X		
2	1	1.00	X				
	2	2.00					X
3	1	1.00	X				
	2	2.00					X
4	1	1.00	X				
	2	2.00					X
5	1	1.00	X				
	2	2.00					X
6	1	1.00	X				
	2	2.00					X
7	1	1.00	X				
	2	2.00					X
8	1	1.00	X				
	2	2.00					X
10	1	1.00	X				
	2	2.00					X
15	1	1.00	X				
	2	2.00					X
20	1	1.00	X				
	2	2.00					X
30	1	1.00	X				

	2	2.00							X
60	1	1.00	X						
	2	2.00							X
120	1	1.00	X						
	2	2.00							X
Minimum gelation concentration: 2 mg.mL^{-1}									

PEP2									
From previous data: < 10min									
Time (min)	Sample	Concentration (mg.mL^{-1})	State						
			Liquid		Liquid / viscous		Viscous	Viscous / solid	Solid
1	1	1.00	X						
	2	1.50			X				
	3	2.00						X	
2	1	1.00	X						
	2	1.50						X	
	3	2.00							X
3	1	1.00	X						
	2	1.50							X
	3	2.00							X
4	1	1.00	X						
	2	1.50							X
	3	2.00							X
5	1	1.00	X						
	2	1.50							X
	3	2.00							X
6	1	1.00	X						
	2	1.50							X
	3	2.00							X
7	1	1.00	X						
	2	1.50							X
	3	2.00							X
8	1	1.00	X						
	2	1.50							X
	3	2.00							X
9	1	1.00	X						
	2	1.50							X
	3	2.00							X
10	1	1.00	X						
	2	1.50							X

	3	2.00	X
Minimum gelation concentration: 1,5 mg.mL^{-1}			

PEP2-RGD							
Previous data unavailable							
Time (min)	Sample	Concentration (mg.mL^{-1})	State				
			Liquid	Liquid / viscous	Viscous	Viscous / solid	Solid
1	1	1.00	X				
	2	2.00	X				
	3	3.00	X				
	4	10.00	X				
2	1	1.00	X				
	2	2.00	X				
	3	3.00	X				
	4	10.00	X				
3	1	1.00	X				
	2	2.00	X				
	3	3.00	X				
	4	10.00	X				
4	1	1.00	X				
	2	2.00	X				
	3	3.00	X				
	4	10.00	X				
5	1	1.00	X				
	2	2.00	X				
	3	3.00	X				
	4	10.00	X				
6	1	1.00	X				
	2	2.00	X				
	3	3.00	X				
	4	10.00	X				
7	1	1.00	X				
	2	2.00	X				
	3	3.00	X				
	4	10.00	X				
10	1	1.00	X				
	2	2.00	X				
	3	3.00	X				
	4	10.00	X				
15	1	1.00	X				

	2	2.00	X
	3	3.00	X
	4	10.00	X
20	1	1.00	X
	2	2.00	X
	3	3.00	X
	4	10.00	X
60	1	1.00	X
	2	2.00	X
	3	3.00	X
	4	10.00	X
Minimum gelation concentration: -			
Note: overall all the samples stay in liquid state but clumping occurs for every concentrations on the first minute			

PEP2/ PEP2-RGD									
Mass ratio 1:1									
Previous data unavailable									
Time (min)	Sample	Concentration ($mg.mL^{-1}$)	PEP2($mg.mL^{-1}$)	PEP2-RGD ($mg.mL^{-1}$)	State				
					Liquid	Liquid/ viscous	Viscous	Viscous / solid	Solid
1	1	2.00	1.00	1.00	X				
	2	3.00	1.50	1.50		X			
	3	5.00	2.50	2.50			X		
2	1	2.00	1.00	1.00	X				
	2	3.00	1.50	1.50		X			
	3	5.00	2.50	2.50				X	
3	1	2.00	1.00	1.00	X				
	2	3.00	1.50	1.50		X			
	3	5.00	2.50	2.50				X	
4	1	2.00	1.00	1.00	X				
	2	3.00	1.50	1.50		X			
	3	5.00	2.50	2.50				clumpy	
5	1	2.00	1.00	1.00	X				
	2	3.00	1.50	1.50		clumpy			
	3	5.00	2.50	2.50				clumpy	
6	1	2.00	1.00	1.00	X				
	2	3.00	1.50	1.50		clumpy			
	3	5.00	2.50	2.50				clumpy	
7	1	2.00	1.00	1.00	X				
	2	3.00	1.50	1.50		clumpy			

	3	5.00	2.50	2.50				clumpy	
10	1	2.00	1.00	1.00	X				
	2	3.00	1.50	1.50		clumpy			
	3	5.00	2.50	2.50				clumpy	
60	1	2.00	1.00	1.00	X				
	2	3.00	1.50	1.50		clumpy			
	3	5.00	2.50	2.50				clumpy	
Minimum gelation concentration: -									
Note: overall all the samples stay in liquid state but clumping occurs for every concentrations									

PEP2/ PEP2-RGD									
Mass ratio 2:1									
Previous data unavailable									
Time (min)	Sample	Concentration ($mg.mL^{-1}$)	PEP2($mg.mL^{-1}$)	PEP2-RGD ($mg.mL^{-1}$)	State				
					Liquid	Liquid/ viscous	Viscous	Viscous / solid	Solid
1	1	2.00	1.33	0.60	X				
	2	3.00	2.00	1.00				X	
	3	5.00	3.33	1.67				X	
2	1	2.00	1.00	0.60	X				
	2	3.00	1.50	1.00					X
	3	5.00	2.50	1.67					X
3	1	2.00	1.00	0.60	X				
	2	3.00	1.50	1.00					X
	3	5.00	2.50	1.67					X
4	1	2.00	1.00	0.60	X				
	2	3.00	1.50	1.00					X
	3	5.00	2.50	1.67					X
5	1	2.00	1.00	0.60	X				
	2	3.00	1.50	1.00					X
	3	5.00	2.50	1.67					X
6	1	2.00	1.00	0.60	clumpy				
	2	3.00	1.50	1.00					X
	3	5.00	2.50	1.67					X
7	1	2.00	1.00	0.60	clumpy				
	2	3.00	1.50	1.00					X
	3	5.00	2.50	1.67					X
10	1	2.00	1.00	0.60	clumpy				

	2	3.00	1.50	1.00	X
	3	5.00	2.50	1.67	X
60	1	2.00	1.00	0.60	clum py
	2	3.00	1.50	1.00	X
	3	5.00	2.50	1.67	X
Minimum gelation concentration: 3mg.mL^{-1}					
Note: overall all the samples stay in liquid state but clumping occurs for every concentrations					

PEP2/ PEP2-RGD									
Mass ratio 5:1									
Previous data unavailable									
Time (min)	Sample	Concentration (mg.mL^{-1})	PEP2(mg.mL^{-1})	PEP2-RGD (mg.mL^{-1})	State				
					Liquid	Liquid / viscous	Viscous	Viscous / solid	Solid
1	1	2.00	1.67	0.30	X				
	2	3.00	2.50	0.50					X
	3	5.00	4.17	0.83					X
2	1	2.00	1.67	0.30	X				
	2	3.00	2.50	0.50					X
	3	5.00	4.17	0.83					X
3	1	2.00	1.67	0.30				X	
	2	3.00	2.50	0.50					X
	3	5.00	4.17	0.83					X
4	1	2.00	1.67	0.30					X
	2	3.00	2.50	0.50					X
	3	5.00	4.17	0.83					X
5	1	2.00	1.67	0.30					X
	2	3.00	2.50	0.50					X
	3	5.00	4.17	0.83					X
6	1	2.00	1.67	0.30					X
	2	3.00	2.50	0.50					X
	3	5.00	4.17	0.83					X
7	1	2.00	1.67	0.30					X
	2	3.00	2.50	0.50					X
	3	5.00	4.17	0.83					X
10	1	2.00	1.67	0.30					X
	2	3.00	2.50	0.50					X

	3	5.00	4.17	0.83	X
60	1	2.00	1.67	0.30	X
	2	3.00	2.50	0.50	X
	3	5.00	4.17	0.83	X
Minimum gelation concentration: 3mg.mL^{-1}					
Note: overall all the samples stay in liquid state but clumping occurs for every concentrations					